VERTEBRATE ZOOLOGY

70 (4): 731 – 756
2020

SENCKENBERG

A critically endangered new species of polymorphic stream frog (Anura: Hylidae: *Atlantihyla*) from the montane rainforest of Refugio de Vida Silvestre Texiguat, Honduras

Josiah H. Townsend[1,2,*], Luis A. Herrera-B.[3], Erich P. Hofmann[1,4], Ileana R. Luque-Montes[1,2], Ayla N. Ross[1], Daniel Dudek, Jr.[1,5], Catherine Krygeris[1,6], Joseph E. Duchamp[1] & Larry David Wilson[2,7]

[1] Department of Biology, Indiana University of Pennsylvania, Indiana, Pennsylvania 15705 – 1081, USA; josiah.townsend@iup.edu — [2] Centro Zamorano de Biodiversidad, Escuela Agrícola Panamericana Zamorano, Departamento de Francisco Morazán, Honduras — [3] Departamento de Biología, Universidad Nacional Autónoma de Honduras en el Valle de Sula, San Pedro Sula, Honduras — [4] Current Address: Science Department, Cape Fear Community College, Wilmington, North Carolina, 28401, USA — [5] Department of Biology, University of Texas at Arlington, Arlington, Texas, 76019, USA — [6] Department of Life and Physical Sciences, Mardela High School, 24940 Delmar Road, Mardela Springs, Maryland 21837, USA — [7] 16010 SW 207th Avenue, Miami, Florida 33187 – 1056, USA

Submitted February 25, 2020.
Accepted November 3, 2020.
Published online at www.senckenberg.de/vertebrate-zoology on November 20, 2020.
Published in print Q4/2020.

Editor in charge: Raffael Ernst

Abstract

The Chortís Highlands of Mesoamerica exhibit a high degree of *in situ* evolutionary diversification, exemplified by numerous endemic radiations of stream-dwelling treefrogs (Anura: Hylidae: *Atlantihyla*, *Duellmanohyla*, and *Ptychohyla*), which have been a source of ongoing taxonomic uncertainty. Recent evidence suggests that one species, *Atlantihyla spinipollex*, may conceal an unrecognized sister species found in Refugio de Vida Silvestre Texiguat. We applied an iterative integrative taxonomic framework to assess this population within the context of Chortís Highlands populations of *Atlantihyla spinipollex sensu stricto*, *Duellmanohyla salvadorensis*, *D. salvavida*, *D. soralia*, and *Ptychohyla hypomykter*, using both a single locus (mtDNA: 16S) and multilocus (mtDNA: 12S, 16S; nDNA: POMC, RAG-1, Rhodopsin) datasets accompanied by distance- and tree-based species delimitation methods to inform our taxonomy. Samples of *A. spinipollex sensu lato* formed two deeply divergent monophyletic lineages, suggesting that populations from the central and eastern Cordillera Nombre de Dios are conspecific, while the population from Refugio de Vida Silvestre Texiguat represents a previously undescribed species. We analyzed morphological and bioacoustic variation within and between the two lineages of *A. spinipollex sensu lato* and found support for recognition of two distinct taxa. We restricted the name *A. spinipollex* to populations in the central and eastern Cordillera Nombre de Dios, and formally describe the Texiguat population as a new species. We recommend the new species be considered Critically Endangered due to ongoing habitat loss within what remains of its highly restricted natural distribution. This new species joins 26 other endemic species of amphibians and reptiles at Texiguat.

Resumen

Las tierras altas Chortís en Centro América presentan un alto grado de diversificación evolutiva *in situ*, demostrado por un numero de radiaciones endémicas de ranas arborícolas asociadas con ecosistemas lóticos (Anura: Hylidae: *Atlantihyla*, *Duellmanohyla* y *Ptychohyla*), y previamente han sido fuente de incertidumbre. Evidencia reciente sugiere que una especie, *Atlantihyla spinipollex*, podría ocultar un especie hermana no reconocida, en el Refugio de Vida Silvestre Texiguat. Aplicamos un modelo iterativo taxonómico integrativo para evaluar esta población dentro del contexto de las poblaciones de las Tierras Altas Chortís de *Atlantihyla spinipollex sensu stricto*, *Duellmanohyla salvadorensis*, *D. salvavida*, *D. soralia*, y *Ptychohyla hypomykter*, utilizando ambos, conjuntos de datos con locus génicos individuales (mtDNA: 16S) y conjuntos de datos con múltiple loci (mtDNA: 12S, 16S; nDNA: POMC, RAG-1, Rhodopsin), acompañados por métodos de delimitación de especies basados en distancia y arboles filogenéticos. Las muestras de *A. spinipollex sensu lato* formaron dos linajes monofiléticos profundamente divergentes, sugiriendo que las poblaciones del centro y Este de la Cordillera Nombre de Dios son conspecíficas, mientras que la población del Refugio de Vida Silvestre Texiguat representa un linaje a nivel de especie no descrito previamente. Analizamos la variación morfológica y bioacústica dentro y entre los dos linajes de *A. spinipollex sensu lato* y encontramos un fuerte

soporte estadístico para el reconocimiento de dos taxones distintos. Restringimos el nombre *A. spinipollex* a las poblaciónes del centro y el Este de la Cordillera Nombre de Dios, y formalmente describimos la población del Refugio de Vida Silvestre Texiguat como una especie nueva. Recomendamos que la nueva especies sea considerada En Peligro Critico debido a la amenaza inmediata y continua de pérdida de hábitat dentro de su distribución natural altamente restringida. Esta nueva especie se une a otras 26 especies endémicas de anfibios y reptiles en Texiguat.

Key words

Atlantihyla melissa sp. nov., *Atlantihyla spinipollex*, Chortís Block Highlands, Cordillera Nombre de Dios, *Ptychohyla hypomykter*, Refugio de Vida Silvestre Texiguat.

Introduction

The Chortís Block biogeographical province of Central America exhibits a high degree of *in situ* evolutionary diversification, generated by a complex and active geological history (Gutiérrez-García & Vásquez-Domínguez, 2013; Jordan *et al*., 2008; Rogers *et al*., 2002; Townsend, 2014). Chortís-endemic radiations are primarily associated with the highlands and have been documented across a wide range of organisms, including amphibians (Crawford & Smith, 2005; Luque-Montes *et al*., 2018; Rovito *et al*., 2015; Townsend, 2016). One diverse group of amphibians, the treefrogs (Anura: Hylidae: Hylini), have multiple endemic radiations across Mesoamerica, including in the Chortís Highlands (Duellman, 1970, 2001; Duellman *et al*., 2016; Faivovich *et al*., 2005; Wiens *et al*., 2005, 2010).

Recently, an expanded phylogeny of Mesoamerican hylids presented by Faivovich *et al*. (2018) included proposed resolutions for long-standing taxonomic uncertainty involving a number of genera, including paraphyly among stream-associated treefrogs assigned to the genera *Bromeliohyla*, *Duellmanohyla*, and *Ptychohyla* (see Duellman *et al*., 2016: 19 for a recent summary of these issues). Faivovich *et al*. (2018)'s proposed taxonomic revisions had implications for a number of species endemic to the Chortís Block. The enigmatic frog *Ptychohyla salvadorensis* was reassigned to *Duellmanohyla*, while its former congener *P. spinipollex* and its putative sister taxon *P. panchoi* were placed in a new genus: *Atlantihyla*. *Ptychohyla hypomykter*, a species endemic to the Chortís Block, remained a member of the genus *Ptychohyla*, along with *P. euthysanota* and four other species with distributions extralimital to the Chortís Block.

The taxon *Atlantihyla spinipollex* was first described by Schmidt (1936: 45; as "*Hyla spinipollex*") based on a single adult male from the "mountains behind Ceiba, Atlantida, Honduras," a locality corresponding to the northern slopes of steep mountains south of the coastal city of La Ceiba that now lie within the limits of Parque Nacional (PN) Pico Bonito (Fig. 1). This species was proposed for inclusion in the genus *Ptychohyla* by Stuart (1954: 169), and subsequent workers considered highland frogs from western Guatemala to northern Nicaragua to represent a single widespread species, *Ptychohyla* (=*Atlantihyla*) *spinipollex* (Duellman, 1963, 1970; Stuart, 1943, 1948; Wilson & McCranie, 1989). Duellman (1963, 1970) noted differences between populations from Honduras and Guatemala and suggested further work might reveal them to represent distinct species, a hypothesis subsequently supported by phylogenetic evidence (Faivovich *et al*., 2018).

Ptychohyla merazi was described by Wilson & Mc Cranie (1989) on the basis of morphological differences between a collection of stream treefrogs from the Quebrada de Oro area on the southeastern side of PN Pico Bonito and *Ptychohyla* from the rest of Honduras, which, at the time, were recognized under a broad concept of *P.* (= *A.*) *spinipollex*. Further evaluation by McCranie & Wilson (1993) revealed that populations found throughout the Cordillera Nombre de Dios (then known to include Refugio de Vida Silvestre [RVS] Texiguat and PN Capiro y Calentura, in addition to PN Pico Bonito) were distinct from highland populations from the rest of Honduras, and subsequently 1) restricted the name *P.* (= *A.*) *spinipollex* to populations from the Cordillera Nombre de Dios, 2) synonymized *P. merazi* with *P.* (= *A.*) *spinipollex*, and 3) described the remaining populations from Honduras and Guatemala as *Ptychohyla hypomykter* (Fig. 1). Following the McCranie & Wilson (1993) concept, *A. spinipollex* was considered to be endemic to three isolated localities in the Cordillera Nombre de Dios: RVS Texiguat, PN Pico Bonito, and PN Capiro y Calentura (McCranie & Wilson, 2002), and was recently discovered at two additional localities: Cerro Corre Viento and PN Nombre de Dios (Townsend & Wilson, 2016).

Despite decades of confusion regarding the taxonomic status of Nuclear Central American populations of frogs presently assigned to *A. spinipollex* and *P. hypomykter*, and long-standing questions as to the monophyly of populations of *P. hypomykter* found across the highlands of Honduras and Guatemala (Duellman, 1963, 1970; McCranie & Wilson, 2002; Faivovich *et al*., 2005, 2018), there has been no phylogenetic analysis to date that includes comprehensive sampling of populations assigned to any of the aforementioned taxa. In an analysis of COI barcodes from amphibians of the Cordillera Nombre de Dios, Townsend & Wilson (2016) demonstrated that samples assigned to *A. spinipollex* from

RVS Texiguat formed a deeply divergent sister clade to *A. spinipollex* from the vicinity of the type locality (PN Pico Bonito) — 14.1–16.5% divergence for COI — and suggested additional investigation was needed to assess the taxonomic status of this population.

In this paper, we take an iterative approach to assessing the systematics of *A. spinipollex sensu lato*, in which we 1) use single-locus (16S rRNA) barcoding to make preliminary taxonomic assignments and identify redundant haplotypes for an ingroup consisting of 114 novel samples of *Atlantihyla*, *Duellmanohyla*, and *Ptychohyla* from the Chortís Highlands; 2) use a subset of the aforementioned samples supplemented with additional sequence data from the mitochondrial gene 12S rRNA and nuclear genes proopiomelanocortin A (POMC), recombination activating gene 1 (RAG-1) and rhodopsin (RHO), and a more broadly sampled comparative dataset, to estimate the phylogenetic relationships of *A. spinipollex sensu lato* among; 3) evaluate the morphological systematics of populations assigned to *A. spinipollex sensu lato*, and 4) formally describe a critically endangered new species endemic to the environs of RVS Texiguat, Honduras, an imperiled endemism hotspot in need of active and immediate conservation measures.

Materials and methods

Taxon Sampling

Specimens and associated tissue samples used in this study were collected during 2008–2018, with fieldwork completed under a series of research permits issued to JHT by the Instituto Nacional de Conservación y Desarrollo Forestal, Áreas Protegidas y Vida Silvestre [ICF] (Resolución GG-MP-055-2006 and Dictamen DAPVS 0091-2006; Resolución DE-MP-086-2010 and Dictamen DVS-ICF-045-2010; Resolución DE-MP-095-2014 and Dictamen ICF-DVS-112-2014; Resolution DE-MP-065-2018 and Dictamen DVS-ICF-008-2018). Research involving amphibians was approved under a series of protocols from the University of Florida IFAS-Animal Research Committee (ARC) and Indiana University of Pennsylvania Institutional Animal Use and Care Committee (IACUC). Field sampling was primarily carried out at night, with searches focused on stream-associated microhabitats. Voucher specimens collected were preserved in 10% formalin and subsequently transferred to 70% ethanol for long-term storage. Vouchers were deposited in the Carnegie Museum of Natural History (CM), Florida Museum of Natural History (UF), National Museum of Natural History, Smithsonian Institution (USNM), Museo de Historia Natural, Universidad Nacional Autónoma de Honduras, Tegucigalpa (UNAH), and Museo de Historia Natural, Universidad Nacional Autónoma de Honduras en el Valle de Sula (UVS); these and other institutional abbreviations follow those standardized by the American Society of Ichthyologists and Herpetologists (Sabaj Peréz, 2016), with the addition of the following abbreviations: IRL (Ileana R. Luque-Montes field series), JHT (Josiah H. Townsend field series), JS (Javier Sunyer field series), MMF (Isis Melissa Medina-Flores field series), and N (2006–08 Nicaragua field series of Scott Travers, Javier Sunyer, Josiah Townsend, and Larry Wilson). Field-collected tissue samples were preserved in SED buffer (20% DMSO, 0.25 M EDTA, pH 7.5, NaCl saturated; Seutin *et al*., 1991; Williams, 2007). Forest formation definitions follow those of Holdridge (1967) and names of forest types, biogeographic regions, and mountains ranges that appear capitalized follow those defined in Townsend (2014).

DNA extraction, PCR amplification, and sequencing

We selected loci for use in phylogenetic analyses to facilitate comparability of our dataset with previously published studies (Duellman *et al*., 2016; Faivovich *et al*., 2005, 2018), choosing to sequence fragments of the mitochondrial genes 12S rRNA and 16S rRNA, and the nuclear protein-coding genes proopiomelanocortin A (POMC), recombination activating gene 1 (RAG-1) and rhodopsin (RHO). A 16S-only dataset containing all available samples of *Atlantihyla*, *Duellmanohyla*, and *Ptychohyla* was used for initial analyses and taxonomic assignment and identification of redundant mitochondrial haplotypes. Based on prior evidence from the more variable barcode marker COI (Townsend & Wilson, 2016), we selected the more conservative 16S for use in preliminary species delimitation, a marker which has been much more broadly sampled for Mesoamerican hylids (Faivovich *et al*., 2005, 2018). Subsequently, a subset of representative samples for each taxon was sequenced for 12S, POMC, RAG-1, and RHO, for inferring the evolutionary relationships of *A. spinipollex sensu lato*. Template DNA was extracted from muscle tissue using the Qiagen PureGene DNA Isolation Kit (Valencia, California, USA) following manufacturer's instructions. Fragments of the mitochondrial gene 12S were amplified using the primers 12SJ-L and 12SK-H (Goebel *et al*., 1999) and 16S using 16Sar-L and 16Sbr-H (Palumbi *et al*., 1991); fragments of the nuclear protein-coding genes POMC were amplified using POMC-3 and POMC-4 (Wiens *et al*., 2005), RAG-1 using R1-GFF and R1-GFR (Faivovich *et al*., 2005), and RHO using Rhod1A and Rhod1C (Bossuyt & Milinkovitch, 2000). Amplification was carried out in 25µL-volume reactions with the following thermocycling parameters: 12S: 2 min at 94°C, 45s at 50°C, and 2 min at 72°C, followed by 39 cycles of: 94°C for 30s, 50°C for 45s, and 72°C for 90s, with a final extension of 10 min at 72°C; 16S: 3min at 94°C, followed by 35 cycles of 45s at 94°C, 45s at 50°C, and 45s at 72°C, with a final extension of 5 min at 72°C; POMC: 2 min at 94°C, followed by 45 cycles of: 94°C for 30s, 56°C for 30s, and 72°C for 1 min, with a final extension

of 7 min at 72°C; RAG-1: 2 min at 94°C, followed by 45 cycles of 30s at 94°C, 30s at 56°C, and 60s at 72°C, with a final extension of 7 min at 72°C; RHO: 5 min at 95°C, followed by 40 cycles of 30s at 95°C, 40s at 60°C, and 90s at 72°C, with a final extension of 5 min at 72°C. PCR products were verified using electrophoresis on a 1.5% agarose gel stained with ethidium bromide. Unincorporated nucleotides were removed from PCR products using 1–2 uL of *ExoSAP-IT* (USB, Santa Clara, CA, USA) per 10uL of PCR product. Each locus and sample was sequenced for both directions; some 16S sequence data were obtained at the Smithsonian Institution Laboratory of Analytical Biology (Suitland, Maryland, USA), and remaining 16S, 12S, POMC, RAG-1, and RHO sequence data were prepared in the Townsend Lab at Indiana University of Pennsylvania and sequenced at Eurofins MWG Operon (Louisville, Kentucky, USA). We obtained reference sequences from GenBank (https://www.ncbi.nlm.nih.gov/genbank) and the alignment provided in the supplemental materials of Faivovich *et al*. (2018). All novel sequences generated for this study were deposited in GenBank (accession numbers MK176937–177076, MH177722–177747); details of samples used in phylogenetic analyses are provided in Appendix 1; alignments used in phylogenetic analyses are provided in Supporting Information.

Molecular systematics

We aligned sequences using clustalw (Thompson *et al*., 1994) as implemented in the program mega7 (Kumar *et al*., 2016). Maximum likelihood (ML) and Bayesian Inference (BI) phylogenetic analyses were performed on 16S-only and mtDNA+nDNA datasets. Analyses of the 16S-only dataset used a final alignment of 134 sequences with a maximum length of 582 bp, consisting of 114 novel sequences of *Atlantihyla spinipollex* (n=14), *A*. sp. nov. (n=24), *Duellmanohyla salvavida* (n=19), *D. soralia* (n=1), *P. euthysanota* (n=1), and *P. hypomykter* (n=55), along with 20 reference sequences (Appendix 1). For analyses of the concatenated mtDNA+nDNA (12S, 16S, POMC, RAG-1, RHO) dataset, we used a final alignment of 34 sequences with a maximum length of 2,628 bp, consisting of 13 novel samples of *A. spinipollex* (n=2), *A*. sp. nov. (n=4), *Duellmanohyla salvavida* (n=2), *D. soralia* (n=1), *D. salvadorensis* (n=2), and *P. hypomykter* (n=2), along with 21 reference sequences (Appendix 1).

Maximum likelihood was performed in raxml v8.2.11 (Stamatakis, 2014), consisting of 2,000 pseudoreplicates using the ML + rapid bootstrap algorithm under the GTR+GAMMA+I model of nucleotide substitution, with the dataset partitioned by gene (12S and 16S) and by codon (POMC, RAG-1, RHO). Prior to Bayesian phylogenetic analysis, we used partitionfinder v1.1.1 (Lanfear *et al*., 2012) to select optimal substitution models for each gene (12S, 16S) and each codon (POMC, RAG-1, RHO), using the "*greedy*" algorithm and "*mrbayes*" set of models, and evaluating the best model using Akaike Information Criterion scores: GTR+I+G was selected for 12S, SYM+I+G for 16S; GTR for POMC codon 1, HKY for POMC codon 2, and GTR for POMC codon3; JC+I for RAG-1 codon 1, HKY for RAG-1 codon 2, HKY+G for RAG-1 codon 3; HKY for RHO codon 1, JC for RHO codon 2, and F81 for RHO codon 3. Bayesian inference was performed using mrbayes 3.2.6 (Huelsenbeck & Ronquist, 2001; Ronquist & Huelsenbeck, 2003), and consisted of two parallel runs of four Markov chains (three heated, one cold) run for 10×10^6 generations and sampled every 1,000 generations, with a random starting tree and the first 4×10^6 generations discarded as burnin.

We applied two methods to the single-locus 16S dataset to aid in species delimitation: Automated Barcode Gap Discovery (ABGD; Puillandre *et al*., 2012), a distance-based approach; and a single threshold general mixed Yule coalescent model (GMYC; Pons *et al*., 2006; Fujisawa & Barraclough, 2013), a tree-based method. The ABGD analysis was conducted using the Kimura (K80) TS/TV substitution model, intraspecific divergence values left at default, 0.001 and 0.1, number of steps equal to 15, and a relative gap width equal to 1.0, all of which was implemented on the ABGD web server (http://www.abi.snv.jussieu.fr/public/abgd/abgdweb.html). We then applied two evaluations of the ABGD results: one using a conservative assessment (= ABGD-CA) with the initial consistent partition as a baseline, to represent the fewest possible species; and a second moderate assessment (= ABGD-MA) using the recursive partition to represent the most frequently occurring partition and a higher number of species groupings. A single threshold GMYC analysis was performed on the Exelixis Lab GMYC web server (https://species.h-its.org/gmyc), which implements the original R code of the GMYC model on a backend server. The input ultrametric tree was generated using beast2 (Bouckaert *et al*., 2014) implementing the Yule speciation model, strict molecular clock, and the reversible jump (RB) substitution model. A chain length of 10^6, while logging parameter values and trees every 1,000 generations, yielded ESS values greater than 200 for all parameters.

Morphological systematics

We examined 76 preserved adults and three metamorphs of *Atlantihyla spinipollex sensu lato*, representing the five known populations: RVS Texiguat (23; Dept. Atlántida: La Liberación, 1030 m a.s.l.: USNM 578651, 578653, 578665–75, 578679–81, 578685–88; Dept. Atlántida: Cerro El Chino, 1390–1430 m a.sensu lato: USNM 578682–83; Dept. Yoro: 2.5 km NNE of La Fortuna, 1550 m), PN Pico Bonito (41; Dept. Atlántida: Quebrada de Oro, 800–1210 m a.s.l.: USNM 514351–56, 514358–92, 578664), PN Nombre de Dios (1; Dept. Atlántida: trail above Roma, 890 m), PN Capiro y Calentura (3 metamorphs; USNM 514394–96), and Cerro Corre

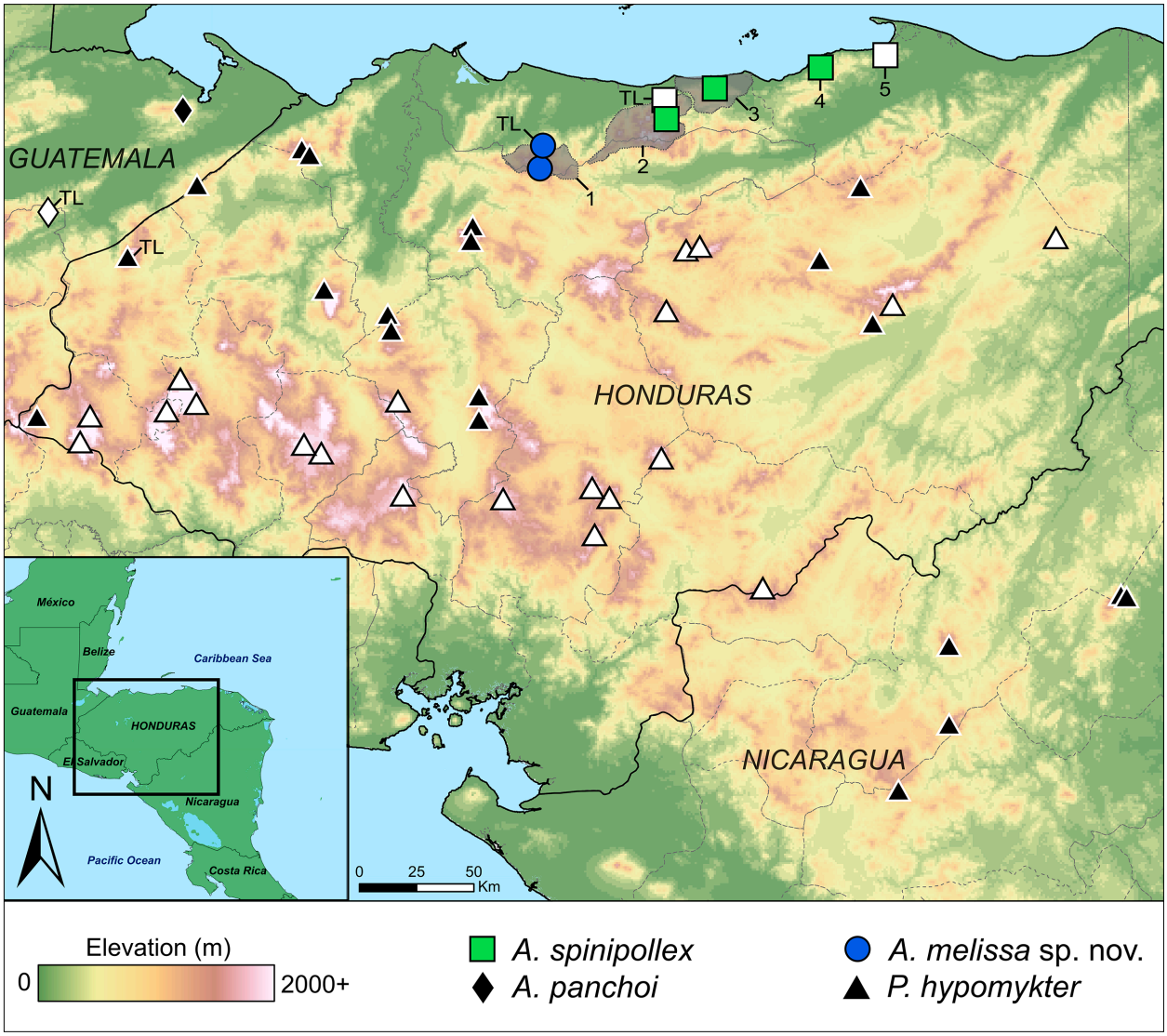

Fig. 1. The known distribution of focal taxa in the Chortís Block. Filled shapes indicate localities with molecular (at least 16S) sequence data generated or utilized herein; additional historical records (with no sequence data) are indicated by white shapes. Numbers and gray-shaded areas refer to relevant localities within the Cordillera Nombre de Dios as follows: 1 = Refugio de Vida Silvestre Texiguat; 2 = Parque Nacional Pico Bonito; 3 = Parque Nacional Nombre de Dios; 4 = Cerro Corre Viento; 5 = Parque Nacional Capiro y Calentura. TL = type locality.

Viento (12; Dept. Colón: Cabaceras Río Manatí Creek, 930–1120 m a.s.l.: CM 170519–30).

Examination and image capture associated with measurements, counts of nuptial spines, and other characterizations were completed using a stereomicroscope and AMScope MU900 microscope eyepiece camera with the software ToupView. Color names and numbers used in the description follow Köhler (2012). Morphological measurements were taken using a digital caliper and rounded to the nearest 0.1 mm. The following measurements were taken of each specimen: snout-vent length (SVL), shank length (SHL; hind limb segment between the knee and the heel), foot length (FL; distance from posterior-most portion of inner metatarsal tubercle to tip of longest toe), head length (HL; tip of snout to posterior angle of jaw), head width (HW; greatest width), width of upper eyelid (EW; perpendicular to outer edge of eyelid), inter-orbital distance (IOD; measured at midlength of upper eyelids), tympanum length (TPL), eye length (EL; horizontal length of eye at widest point, measured inside margin of eyelid), and third finger disc width (DW; measured ventrally at widest point between outer edges of disc covers). Differences between the observed mean values for measurements from each taxon and sex were calculated with a comparison of means test, which calculates a significance value (p) representing the probability of obtaining the observed means if the difference between them is zero.

We performed Principal Component Analyses (PCA) on morphological measurements in R 3.4.1 (R Core Team, 2017) to determine if variation in morphology could be attributed to the genetic lineages. Forty-one adult males and 35 adult females were included in these analyses, and all analyses were conducted on males and females

separately to account for sexual size dimorphism. Based on the lineage recovered in our phylogenetic analyses, specimens from Corre Viento and Pico Bonito were considered one taxon (*A. spinipollex sensu stricto*) and specimens from the divergent Texiguat lineage as another (*A.* sp. nov.). We first regressed measurements against SVL to account for variation in body size. The data were then scaled to their standard deviation in order to normalize their distribution. PCAs were carried out using '*prcomp*' command in R. The packages *ggfortify* (Tang *et al*., 2016) and *ggplot2* (Wickham, 2016) were used to plot results of analyses. Principle component scores are provided in Appendix 2.

Bioacoustic processing and analysis

An audio recording of the advertisement call for a single adult male *Atlantihyla* sp. nov. (UVS V671) collected from the Río Jilamito, Refugio de Vida Silvestre Texiguat, Departamento de Atlántida, was recorded at a laboratory of the Museo de Historia Natural at the Universidad Nacional Autónoma de Honduras en el Valle de Sula (UNAH-VS) on 7 March 2018, at 1635h, as it vocalized inside a large terrarium approximately 24 hours after capture. A video recording of vocalizations was taken of an uncollected adult male *A. spinipollex sensu stricto* from Cerro Corre Viento, Departamento de Colón, on 14 January 2019 at 2239h, as it called from among a group of 10+ other males around a pool at the base of a ca. 8m tall waterfall. The audio component of the video recording (M2TS format; 0:51 in total length; 29.97 frames/s; audio recorded at 192kbps, sampling rate 48,000 Hz) was extracted to an AIF format using Adobe Premiere Pro CC (Adobe Systems Incorporated). Temperature data from the time of recording were not available. Vocalizations were analyzed using Raven Pro 1.5 version 64-bit for Windows (Bioacoustics Research Program, 2014), at a sampling rate of 48,000 Hz and a resolution of 16 bits. Spectral parameters for calls and notes were obtained using a Blackman window, DFT size at 1024 samples, 3 db filter bandwidth 76.9 Hz. Based on the characteristics of the vocalizations, we used a note-centered approach to define our terminology for calls, notes, pulses, and their associated parameters (Köhler *et al*., 2017). We recorded the following spectral and temporal parameters: call duration, note duration, number of notes per call, number of pulses per note, pulse duration, inter-pulse interval, pulse repetition rate (pulse/second), and dominant frequency (Hz) of the call. Given the limitations of the available recordings and the lack of associated temperature data for *A. spinipollex sensu stricto*, we limited our direct comparisons to note duration, pulse count, and dominant frequency, three traits with low intraspecific variability that are minimally influenced by temperature (Köhler *et al*., 2017). Thus, the resulting comparisons were qualitative and not meant to characterize the full range of variation in vocalizations for either population.

Results

Phylogenetic analyses

Analyses of the 16S-only dataset using ABGD (CA and MA) and GMYC yielded somewhat conflicting results for some taxa, with, perhaps predictably, ABGD-CA failing to delimit some closely related nominal species, and ABGD-MA and GMYC recovering species limits consistent with the existing taxonomy and delimiting divergent lineages within recognized taxa into candidate species (Fig. 2). All three analyses unambiguously support delimiting *Atlantihyla spinipollex* into two or more species, with GMYC further delineating eastern and central *A. spinipollex sensu stricto* (as indicated in Fig. 2) into two species, and ABGD-MA splitting *A. spinipollex* sensu lato into five species (Fig. 2). Support for the delimitation of *A. panchoi*, *Duellmanohyla salvavida* and *D. soralia* was unambiguous across all three analyses. Within the genus *Ptychohyla*, the most conservative analysis (ABGD-CA) only recognized three species, failing to delimit *P. euthysanota*, *P. hypomykter sensu stricto*, and *P. macrotypanum*, or *P. leonhardschultzei*, *P. zophodes*, and *P.* sp. (an undescribed species from Guatemala first identified in Faivovich *et al*., 2005; Fig. 2). All three analyses recovered *P. cf. hypomykter* (from central Guatemala) as a distinct species from *P. hypomykter sensu stricto* from the Chortís Block (Fig. 2).

The analysis of the mtDNA+nDNA dataset recovered a well-supported *Atlantihyla* clade containing *A. panchoi* and *A. spinipollex sensu lato* as sister to *Ptychohyla* (Fig. 3). The majority of our species-level relationships were otherwise congruent with those of Faivovich *et al*. (2018), which used broader taxonomic and genetic sampling, and largely well-supported (PP > 0.99 for all but one node). A notable exception is *D. salvadorensis*, which is an unresolved and weakly supported sister to the *Atlantihyla-Ptychohyla* clade. This likely an artifact of the lack of sampling from the southern clade of *Duellmanohyla* in our phylogeny, and that the phylogenetic relationships and taxonomic assignment of this species has long been problematic, as evidenced by Faivovich *et al*. (2018) devoting a figure and nearly two pages of text to discussion of this species. Across all analyses, two deeply divergent, reciprocally monophyletic lineages were recovered from samples assigned to *A. spinipollex* from northern Honduras. The first lineage contained samples from PN Pico Bonito (Dept. Atlántida; near the vicinity of the type locality), PN Nombre de Dios (Dept. Atlántida), and Cerro Corre Viento (Dept. Colón). Given that this lineage contains material collected near the type locality of *A. spinipollex*, we consider these samples to represent *A. spinipollex sensu stricto*. The second lineage consisted of samples from RVS Texiguat (Depts. Atlántida and Yoro), which we refer to as *A.* sp. nov. Mitochondrial pairwise distances were relatively high between these lineages and demonstrated a wide gap between intraspecific and interspecific distances, ranging from

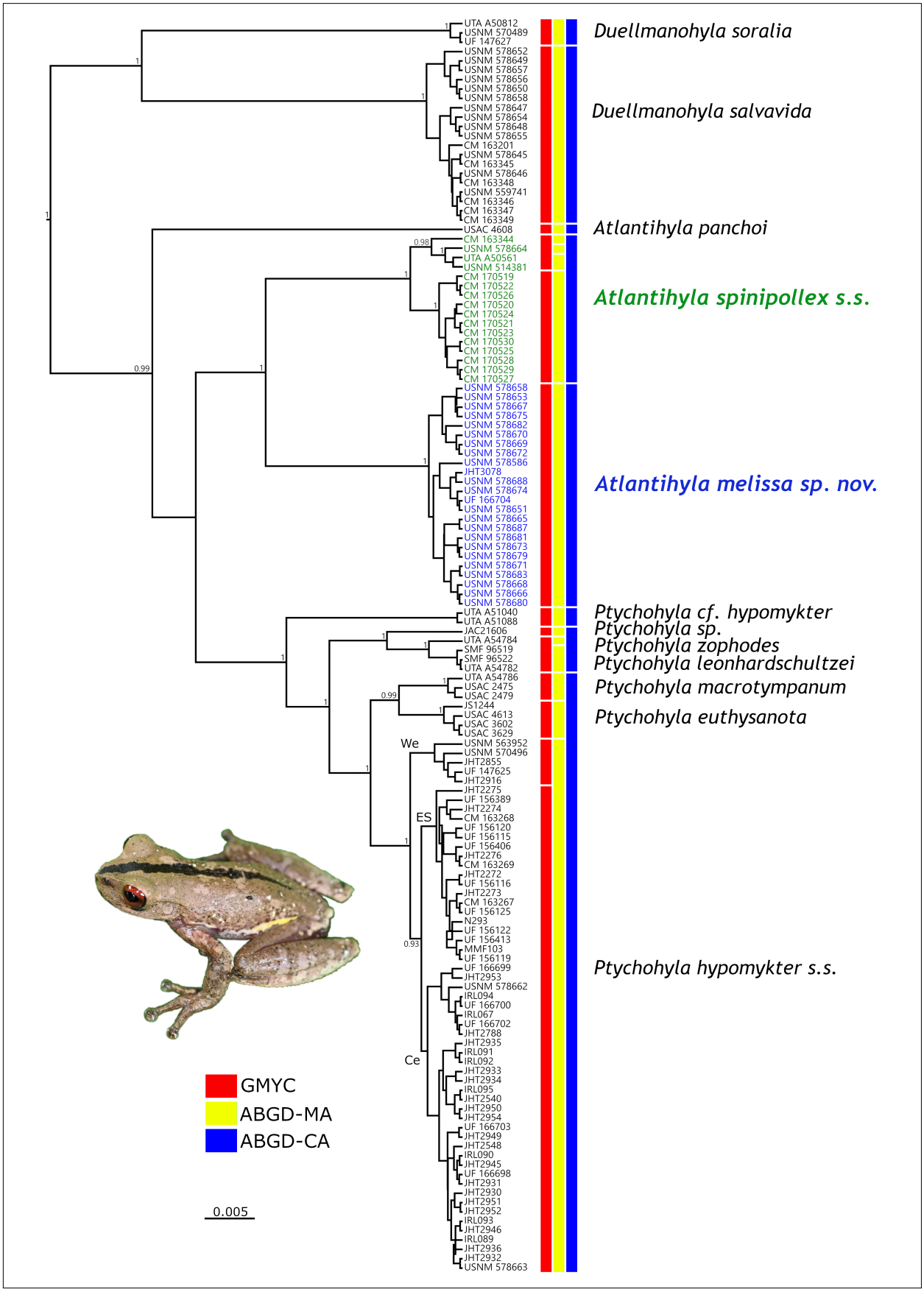

Fig. 2. Bayesian ultrametric tree based on 16S mitochondrial dataset, showing inferred species limits from tree-based (GMYC) and distance-based (ABGD-MA and ABGD-CA thresholds) analyses. Bayesian posterior probabilities (≥0.9) for nodes corresponding to lineages delimited in the analyses are shown above corresponding branches. Geographic haplogroups of *Ptychohyla hypomykter* labeled as follows: We = Western, Ce = Central, and ES = Eastern-Southern. Photo of paratype (USNM 578672) of *A. melissa* (© JHT).

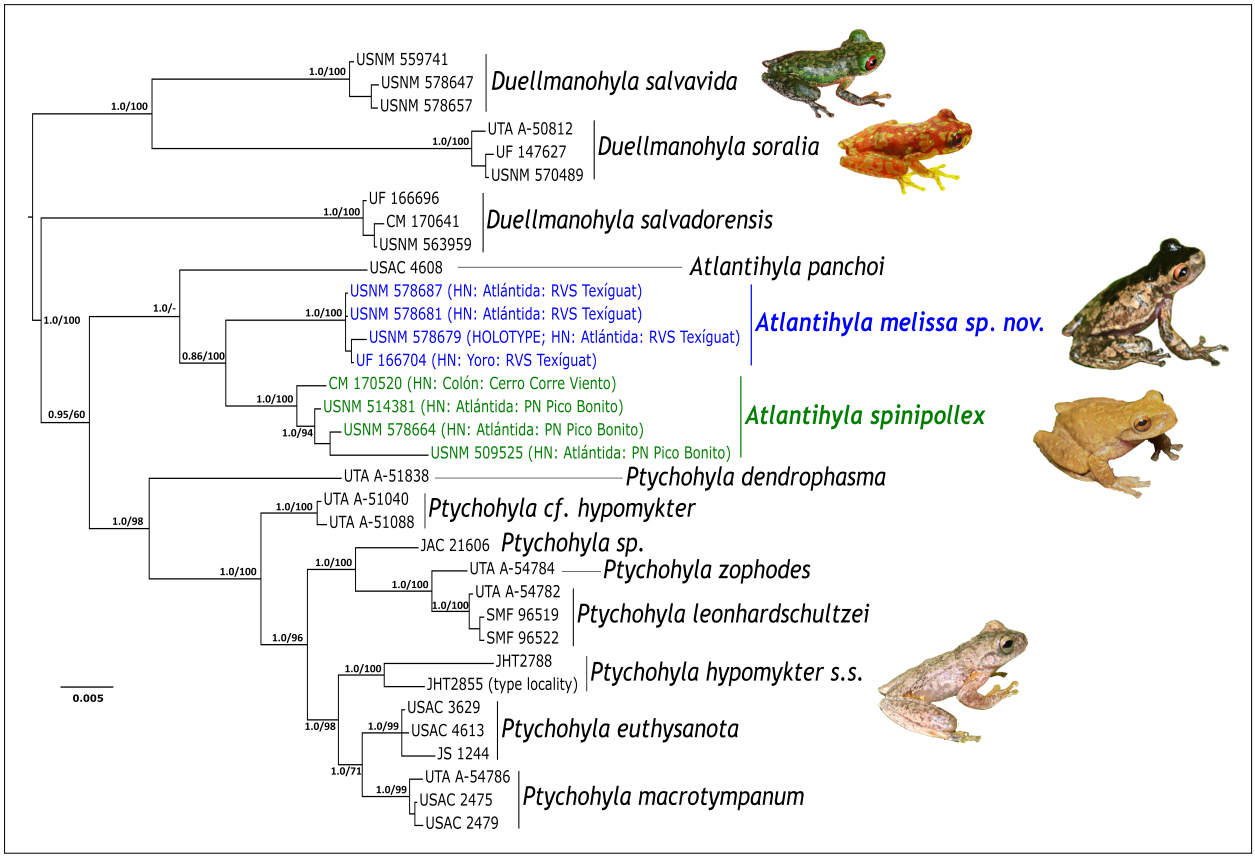

Fig. 3. Multilocus Bayesian phylogram based on combined mtDNA (12S, 16S) + nDNA (POMC, RAG-1, RHO) dataset; maximum likelihood bootstrap support values (0–100) and Bayesian posterior probabilities (0–1.0) shown above corresponding branches. Photos from top to bottom: *D. salvavida* from Río Jilamito, Dept. Atlántida, Honduras © JHT; *D. soralia* from Merendón, Dept. Cortés, Honduras © JHT; holotype of *A. melissa* © JHT; *A. spinipollex* from Cerro Corre Viento, Dept. Colón, Honduras © Jason M. Butler; *Ptychohyla hypomykter* from Rio Negro de Comayagua, Dept. Comayagua, Honduras (© JHT).

3.8–5.2% for 12S (intralineage distances: *A. spinipollex s.s* 0.0–0.7%; *A.* sp. nov. 0.1%) and 4.1–5.0% for 16S (*A. spinipollex s.s* 0.0–1.2%; *A.* sp. nov. 0.0–0.4%).

Morphological variation

We examined 76 adult specimens and three metamorphs of *Atlantihyla spinipollex sensu lato*, representing the majority of existing museum specimens and including the entire distribution of *A. spinipollex*: nine males and 15 females from RVS Texiguat, 22 males and 19 females from PN Pico Bonito, 10 males and one female from Cerro Corre Viento, and three metamorphs from PN Capiro y Calentura (Appendix 2). Based on our phylogenetic results, we considered the PN Pico Bonito, PN Nombre de Dios, and Cerro Corre Viento populations to represent a single group, *A. spinipollex sensu stricto*, and compared those samples to samples from RVS Texiguat (Table 1, Fig. 4). Both male and female frogs from RVS Texiguat were significantly smaller than *A. spinipollex sensu stricto* (SVL; males: mean difference = 3.05, sd = 0.88, t-stat = 3.451, p = 0.0014, DF = 39; females: mean difference = 5.62, sd = 1.61, t-stat = 3.495, p = 0.0014, DF = 33), had relatively longer shanks (SHL/SVL; males = t-stat –3.683, $p < 0.001$; females t-stat = –4.666, $p < 0.0001$), relatively longer hind feet (FL/SVL; males t-stat = –3.536, p = 0.0011; females t-stat = –3.056, $p < 0.005$), and heads that are longer (HL/SVL; males t-stat = –6.081, $p < 0.0001$; females t-stat = –7.068, $p < 0.0001$) and broader (HW/SVL; males t-stat = –5.902, $p < 0.0001$, DF = 39; females t-stat = –5.988, $p < 0.0001$).

Principal component analyses recovered individuals from *A. spinipollex sensu stricto* and samples from RVS Texiguat as distinct clusters that overlapped somewhat in morphospace (Fig. 5); PCA scores are available in Appendix 3. The first six principal components explained at least 95% of the cumulative variance in both male and females. In males, HW, HL, and SHL (all regressed against SVL) had the strongest positive loadings in PC1 (0.377, 0.370, 0.362, respectively), which accounted for 66.0% of the variation. In females, the same measurements had strong negative loadings in PC1 (–0.368, –0.370, –0.360, respectively), which accounted for 66.7% of the variation. DW/SVL had strong negative loadings in PC2 in both males (–0.772) and females (–0.724). Additionally, in PC2, males exhibited strong negative loadings in EW/SVL (–0.571), while females exhibited strong negative loadings in FL/SVL (–0.501). PC2 accounted for 10.9% of the variation in males, and 15.5% of the variation in females.

Table 1. Comparison of morphological variation between *Atlantihyla melissa* and *A. spinipollex*; range followed by mean and standard error in parentheses.

	Atlantihyla spinipollex		*Atlantihyla melissa*	
	Males (n=32)	Females (n=20)	Males (n=9)	Females (n=15)
SVL	32.9–40.5 (36.24, 2.07)	30.9–45.8 (41.17, 4.57)	30.4–38.8 (33.19, 3.19)	30.9–43.9 (35.55, 4.89)
SHL/SVL	0.474–0.600 (0.520, 0.0276)	0.486–0.568 (0.520, 0.0283)	0.521–0.666 (0.564, 0.0440)	0.497–0.727 (0.594, 0.0632)
FL/SVL	0.368–0.462 (0.417, 0.0281)	0.360–0.486 (0.418, 0.0323)	0.425–0.568 (0.459, 0.0421)	0.408–0.543 (0.457, 0.0433)
HL/SVL	0.312–0.392 (0.348, 0.0187)	0.325–0.381 (0.349, 0.0173)	0.346–0.427 (0.401, 0.0353)	0.367–0.477 (0.409, 0.0324)
HW/SVL	0.309–0.364 (0.327, 0.0139)	0.313–0.370 (0.333, 0.0163)	0.327–0.442 (0.370, 0.0327)	0.345–0.459 (0.382, 0.0315)
EW/IOD	0.555–0.933 (0.717, 0.1002)	0.562–0.891 (0.730, 0.0868)	0.576–0.745 (0.651, 0.0510)	0.064–0.832 (0.750, 0.0624)
TPL/EL	0.375–0.521 (0.460, 0.0485)	0.387–0.526 (0.461, 0.0374)	0.433–0.520 (0.474, 0.0304)	0.425–0.554 (0.486,0.0361)
IOD/EL	0.886–1.251 (1.079, 0.1017)	0.833–1.284 (1.048, 0.1209)	0.915–1.246 (1.054, 0.1102)	0.938–1.256 (1.115, 0.0947)
Nuptial spines	29–62 (46.0, 9.492; n=23)	—	39–53 (45.75, 4.496; n=8)	—

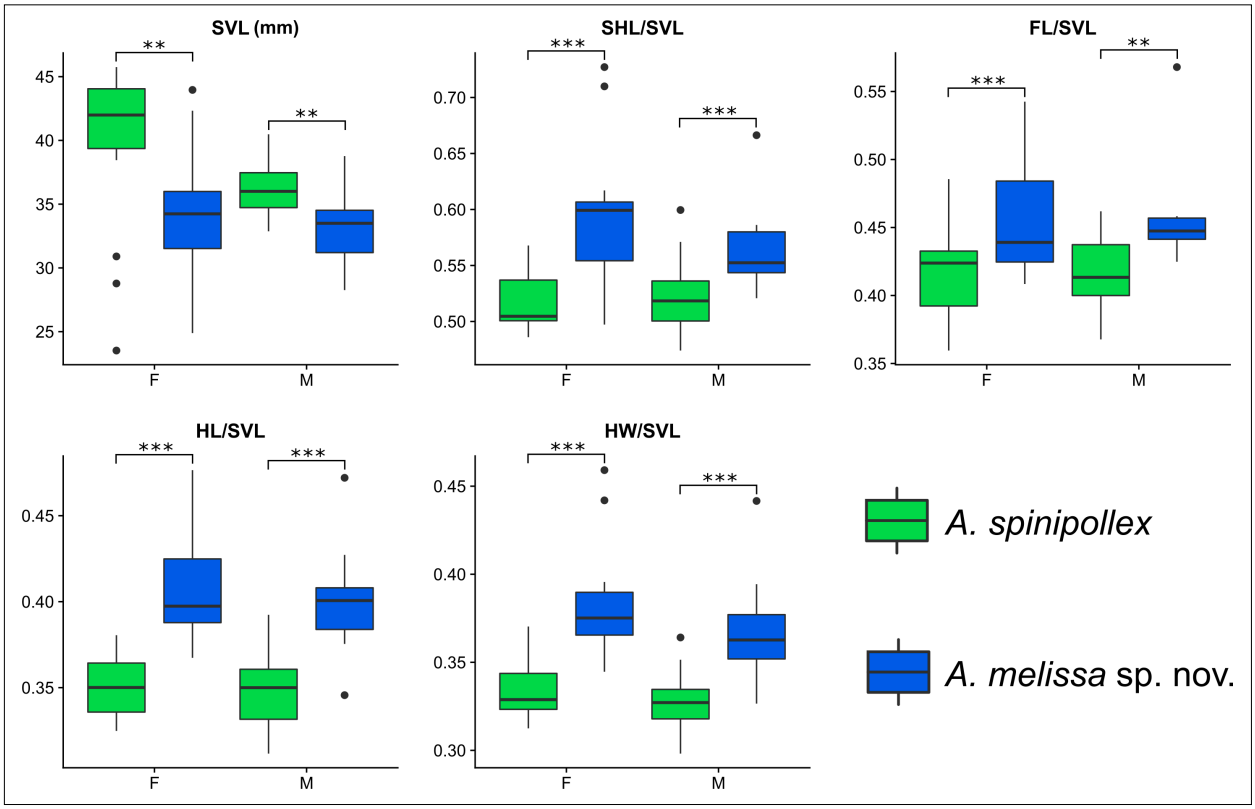

Fig. 4. Direct comparisons of snout-vent length (SVL) and four morphometric ratios between female and male *A. spinipollex* and *A. melissa* sp. nov. SHL = shank length; FL = foot length; HL = head length; HW = head width. Asterisks indicate significant comparisons: ** $p < 0.001$; ** $p < 0.0001$.

Comparative bioacoustics

A recording from a single male *Atlantihyla* sp. nov. from Río Jilamito consisted of a series of four calls, each consisting of series of 5–6 evenly-spaced pulsed notes with a dominant frequency of 3421.9 Hz, with each note having a duration of 0.47–1.3 s (n=16, x=0.913, sd=0.21) and consisting of 5–12 (x=8.21, sd=2.16) pulses per note (Fig. 6). A recording from an intermittently calling male *A. spinipollex sensu stricto* from Corre Viento con-

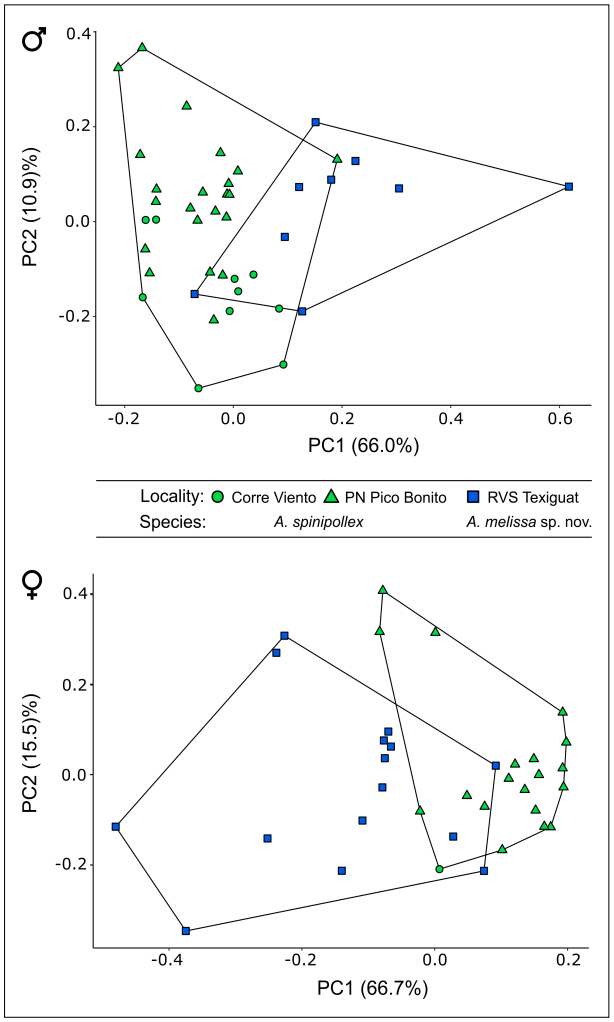

Fig. 5. The first two principal components of morphological characters for males (top) and females (bottom), which accounted for the majority of variation in the analyses.

sisted of a series of five intermittent pulsed notes with a dominant frequency of 3328.1 Hz, and each note having a duration of 0.606–0.752 s (x = 0.669, sd = 0.079) and consisting of 6–7 pulses (x = 6.4, sd = 0.577). It is not apparent if these vocalizations are representative of a complete advertisement call for *A. spinipollex sensu stricto*, as they were intermittent and do not include notes in a series forming a call sequence, as seen in *A.* sp. nov. Due to this difference and the lack of directly comparable call sequence for *A. spinipollex sensu stricto*, we limit the conclusions drawn by direct comparison.

Based on these limited samples, we found that *A.* sp. nov. had a higher dominant frequency than *A. spinipollex* sensu stricto (3421.9 vs. 3328.1 Hz) and the average duration of notes was significantly longer than those of *A. spinipollex sensu stricto* (p = 0.021, t-statistic = −2.505, DF = 20). The pulsed note structures in both samples were similar, with notes of *A.* sp. nov. consisting of relatively more pulses (5–12, x = 8.21, sd = 2.16) than those of *A. spinipollex sensu stricto* (6–7, x = 6.4, sd = 0.577), although the means are not significantly different (p = 0.0541, t-statistic = −2.04, DF = 21).

Systematic description

The results of our molecular and morphological analyses, supplemented by bioacoustic and biogeographic data, provide unambiguous support for recognition of the RVS Texiguat population as a distinct species, which we name

Atlantihyla melissa sp. nov.

ZooBank urn:lsid:zoobank.org:act:A63E72DA-E7B3-4B96-9A6D- FAD52411F624

Figs. 7–8, 11–13

Ptychohyla spinipollex: McCranie *et al*., 1993: 1060.
Ptychohyla spinipollex (in part): McCranie & Wilson, 1993: 100.
Ptychohyla spinnipolex (*sic*, in part): McCranie & Solís, 2013: 242.
Atlantihyla spinipollex (in part): Faivovich *et al*., 2018: 24.

Holotype. USNM 578679 (field number JHT 3114; Figs. 7, 8), an adult male from alongside the Río Jilamito at La Liberación (15.5302°N, 87.2939°W, WGS84; Figs. 9, 10a-c), 1,030 m, Refugio de Vida Silvestre Texiguat, Departamento de Atlántida, Honduras; collected 14 June 2010 by Benjamin K. Atkinson, Cesar A. Cerrato, Luis A. Herrera-B., Mayron McKewy Mejía, Josiah H. Townsend, and Larry David Wilson. GenBank accession numbers: 12S (MK176937), 16S (MK176946), POMC (MK177061), RAG1 (MW177730), RHO (MK177068).

Paratypes. Twenty-one (21) paratopotypes, including eight adult males (USNM 578670, 578674 [Fig. 11e], 578675, 578677, 578680–81, 578685, 578687) and 13 adult females (USNM 578665 [Fig. 11c], 578666–67, 578668 [Fig. 11f], 578669, 578671, 578672 [Fig. 11b], 578673, 578676 [Fig. 11a], 578678, 578682, 578686 [Fig. 11d], 578688), collected between 1,015–1,090 m elevation in the vicinity of the Río Jilamito at La Liberación, Refugio de Vida Silvestre Texiguat, Departamento de Atlántida, Honduras; 10–18 June 2010 and 25–27 June 2010. Two (2) adult female paratypes (USNM 578683–84) from Cerro El Chino (15.5225°N, 87.2802°W), a peak to the ESE of La Liberación, 1,420–1,430 m elevation, Departamento de Atlántida, Honduras, collected 19 June 2010. One (1) adult female paratype (UF 166704) from 2.5 airline km NNE of La Fortuna (15.4328°N, 87.3093°W; Fig. 10d, 10e), 1,610 m elevation, Departamento de Yoro, Honduras, collected 9 April 2008 by Jason M. Butler, John Slapcinsky, Nathaniel Stewart, Josiah H. Townsend, and Larry David Wilson.

Referred specimens. Twenty-seven (27) specimens not included in our molecular or morphological analyses are referred to this species, including one (1) specimen from 3.8 km east and 1.5 km south of Cerro Cabeza de Negro (UNAH 2708), five (5) specimens from the north slope of Cerro Texiguat (UNAH 1470, 1472, 1493, 1893–94), and 14 specimens from Río Jilamito at La Liberación (UVS V669–V682), all localities in Departamento de Atlántida, Honduras; and 12 specimens from approximately 2.5 airline km north-northeast of La Fortuna (UF 142417–21, UNAH 3738, USNM 514397–402), Departamento de Yoro, Honduras.

Diagnosis. The new species is a member of the genus *Atlantihyla*, based on results from the mtDNA+nDNA phylogenetic analyses (Fig. 3) and by possession of a

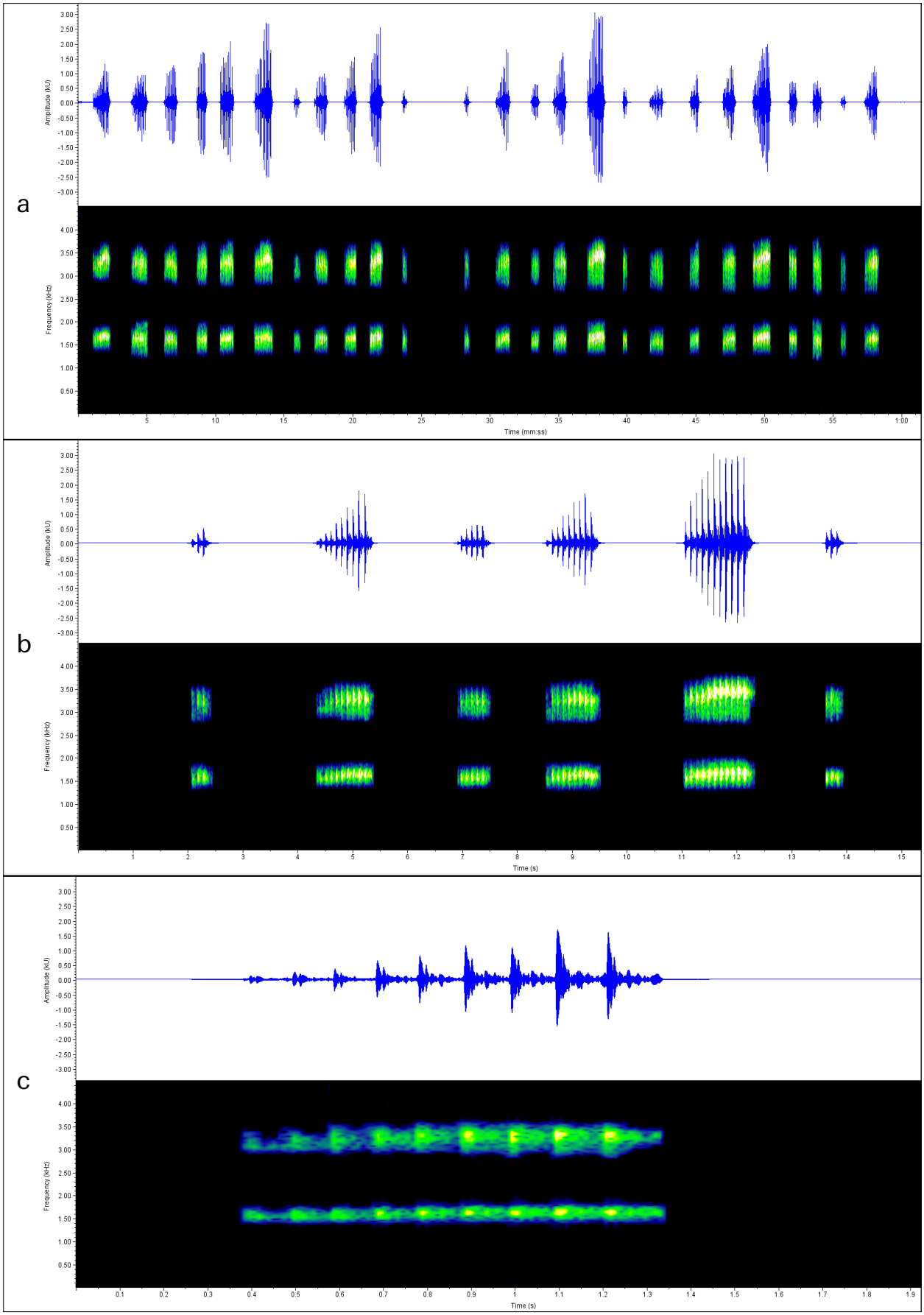

Fig. 6. Advertisement call of an adult male *Atlantihyla melissa* (UVS V671): (**a**) waveform (top) and spectrogram (bottom) of a call series (60 seconds); (**b**) waveform (top) and spectrogram (bottom) of a single call (15 seconds; third call in series above); and (**c**) waveform (top) and spectrogram (bottom) of a single note (1.9 seconds; second note in call above).

vertical rostral keel, as well as enlarged dark-colored spine-shaped epidermal projections on the prepollex and a pale ventrolateral stripe in males (Faivovich *et al*., 2018). *Atlantihyla melissa* can be distinguished from its sister species, *A. spinipollex* (Fig. 4), by having a relatively smaller adult size (adult males 30.4–38.8 mm [33.19 ± 3.186] and adult females 30.9–43.9 mm [35.55 ± 4.89], versus 32.9–40.5 mm [36.24 ± 2.07] and 30.9–45.8 mm [41.14 ± 4.57] in *A. spinipollex*), having relatively longer shanks, a relatively larger head, significantly longer note duration in the advertisement call, and relatively more pulses per note. The only other member of the genus, *A. panchoi*, differs from *A. melissa* in having a well-defined white-lined upper lip (upper lip coloration consistent with adjacent areas or slightly paler in *A. melissa*). *Atlantihyla melissa* is also well differentiated from other taxa on the basis of DNA sequence variation. From its sister species and closest known relative, *A. spinipollex*, the new species has sequence divergences of 3.8–5.2% for 12S and 4.1–5.0% for 16S, and from *A. panchoi*, divergences ranged from 3.8–4.2% for 12S and 5.5–5.7% for 16S. Townsend and Wilson (2016) also reported COI sequence divergence between *A. melissa* (as *Ptychohyla* sp.) and *A. spinipollex* ranging from 14.1–16.5%. The distribution of *A. melissa* is allopatric with respect to *A. panchoi* and *A. spinipollex*.

Atlantihyla melissa is known to occur in sympatry or near-sympatry with four other species of stream-associated hylids: *Duellmanohyla salvavida*, *Isthmohyla insolita*, *Plectrohyla chrysopleura*, and *P. cf. guatemalensis*; and can be distinguished from *D. salvavida* in having a dorsal coloration that can be uniform grayish brown or with varying degrees of light or dark spots or mottling, and large nuptial spines in adult males (dorsum uniform green or occasionally mottled green with tiny nuptial excrescences in *D. salvavida*), from *I. insolita* in having a relatively smooth dorsal surface, patternless or lightly mottled chin coloration, and large nuptial spines in adult males (dorsal surface tuberculate, chin with well-defined pale central blotch resembling a broad stripe, and tiny nuptial excrescences in *I. insolita*), and from *P. chrysopleura* and *P. cf. guatemalensis* in having a prepollex that is only slightly enlarged and lacks a protruding distal end (prepollex enlarged and flat, with blunt distal end in *P. chrysopleura*, prepollex with two large curved spines that protrude from the skin on the distal end in *P. cf. guatemalensis*). Although allopatric in distribution, *Ptychohyla hypomykter* is also known from localities in the Department of Yoro, Honduras, and differs from *A. melissa* in lacking a pale dorsolateral stripe in adult males and in having a thick, rounded tarsal fold (irregular pale dorsolateral stripe, sometimes incomplete, and thin tarsal fold in *A. melissa*).

Description of holotype. An adult male (USNM 578679; Figs. 7, 8) having a snout-vent length of 34.4 mm, tibia length 18.7 mm; tibia length/SVL 0.544; foot length 15.4 mm; foot length/SVL 0.447; head length 13.2 mm; head length/SVL 0.384; head width 12.1 mm; head width/SVL 0.352; eyelid width 3.0 mm; eye length 4.62 mm; tympanum diameter 2.1 mm; tympanum/eye diameter 0.446; inter-orbital distance 4.59 mm; inter-orbital distance/eye length 0.994. Snout truncate in lateral view, rounded in dorsal view; weak vertical rostral ridge present; canthus distinct and rounded; loreal region concave; nostrils slightly protuberant; internarial distance 3.2 mm; top of head flat; supratympanic fold well developed, extending from point 0.4 mm posterior of the eye above tympanum to point above insertion of forearm, contacting to slightly covering upper edge of tympanum; tympanum distinct, rounded. Pupil horizontally elliptical. Forearm somewhat more robust than upper arm, with row of unequally elevated ulnar tubercles forming a ridge on the ventral portion of the forearm. Prepollex ossified and bluntly rounded; finger I of the right hand has 39 dark colored, spine-shaped papillary epidermal projections that are relatively large, well-defined, and juxtaposed to one another in a bell-shaped patch, located on the interior and ventral surfaces of the prepollical area of the digit; subarticular tubercles rounded and globular, distal tubercles on finger III weakly divided and finger IV bifid; discs on fingers large, discs of fingers II and III slightly smaller than diameter of the tympanum; relative length of fingers I<II<IV<III; basal webbing between fingers I and II, webbing formula **II** 1¾–2 ¾ **III** 2^{+}–2 **IV**; unwebbed portions of fingers with lateral keels. Heels overlap when hind limbs adpressed at right angle to body; inner tarsal dermal fold present but weakly defined; outer tarsal fold absent; heel tubercle present; subarticular tubercles on toes rounded, largest on toes I and V; relative toe length I<II<III≈V<IV; webbing formula **I** 1^{+}–2^{-} **II** 1^{+}–2 **III** 1^{+}–2 **IV** 2–1^{+} **V**; unwebbed portions of fingers with lateral keels; toes moderately long; toe discs slightly smaller to about same size as finger discs. Cloacal opening directed posteroventrally at midlevel of thighs, with skin below cloaca featuring several folds radiating out from cloacal opening. Skin on dorsum smooth; skin on throat, chest, belly and ventral surface of thighs weakly granular, with some weak tubercles present on dorsal surfaces of eyelids. Ventrolateral glands absent. Tongue ovoid with faint indication of posterior notch; vomerine teeth, situated on a pair of small, elliptical elevations between ovoid internal nares, with three vomerine teeth on left side and two on right side. Vocal slits present on both sides, vocal sac single, median, subgular.

Measurements of holotype (in mm). SVL 34.44, SHL 18.72, FL 15.41, HL 13.22, HW 12.12, EW 3.01, EL 4.62, IOD 4.59, TPL 2.06.

Colouration of holotype. Colour in life of the adult male holotype (USNM 578679, Fig. 7) is as follows: dorsum of head, body, forelimbs, and hind limbs mottled Light Buff (2) and Chamois (84) with Brownish Olive (276) reticulations and a large, irregular Sepia (286) blotch covering most of the dorsal surface of the head and roughly one half of the body, resembling an ink drop; upper lip mottled Chamois (84), Flesh Color (249), and

Fig. 7. Adult male holotype of *Atlantihyla melissa* (USNM 578679; SVL = 34.4 mm), shown in life (left) and in dorsal (top right) and ventral (bottom right) aspects after eight years in preservation (© JHT).

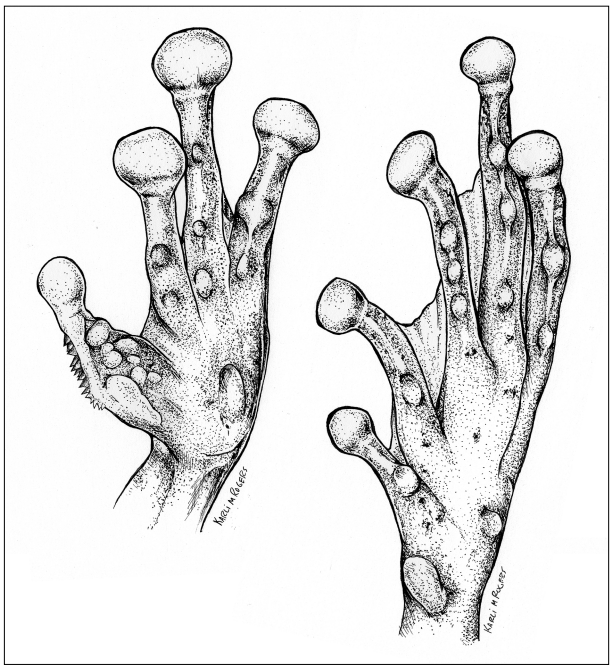

Fig. 8. Semi-diagrammatical illustrations of the ventral aspects of the hand (left) and foot (right) of the holotype of *Atlantihyla melissa* (USNM 578679).

Vinaceous Pink (245), with no indication of labial stripe; ventrolateral stripe Pale Buff (1), well-defined but with somewhat irregular shape, extending from axilla to insertion of hindlimb, creating sharp distinction between dorsal and ventral coloration; ventrolateral stripe bordered ventrally with Pale Purple (223) and Dark Pinkish Rose (220), with scattered Pinkish White (216) granules; venter Pinkish White (216), ventral surfaces of limbs Light Lilac (221) to Lilac (222), Light Buff (2) stripe forming a semicircle above and around the cloaca; iris Salmon Color (83) with some Sepia (286) reticulations.

Variation. *Atlantihyla melissa* exhibits sexual dimorphism in terms of size and coloration. Females are larger than males, with maximum recorded size for males 38.77 mm and females 43.96 mm; the ranges of variation in measurements and relative ratios for males and females are summarized in Table 1. All adult male specimens of *A. melissa* examined were in breeding condition, with patches of relatively large, dark-colored, spine-shaped papillary epidermal projections that are juxtaposed to one another in a roughly bell-shaped patch on the interior surface of each thumb. Nuptial spine counts from the right thumbs of eight adult males number 39–53 (45.75 ± 4.496).

Male and female *A. melissa* exhibit a wide range in variation of coloration and pattern (Figs. 11, 12). Iris color in males ranges from Salmon Color (58) to Flame Scarlet (73); in females, iris color is more subdued, ranging from Tawny Olive (17) to Cinnamon Drab (50). There appears to be no discernable pattern of sexual dimorphism in relation to dorsal and ventral coloration. Variation in dorsal pattern ranges from nearly uniform in coloration (Fig. 12b); extensively mottled (Fig. 11e, 11f, 12d); small to medium-sized irregular dark spots (Fig. 11c, 12a); small pale spots that appear glandular (Fig. 12c); large and irregular "ink spot" botching, similar to that of the holotype (Fig. 12e, 12f); pale irregular blotches (Fig. 11d, 12g); or with a pronounced dark middorsal stripe that can be narrow and well-defined (Fig. 11a, 12j) or broader with irregular borders (Fig. 11b, 12h). Most, but not all, individuals have an indication of a pale ventrolateral stripe, which can be Pale Buff (1), Cream Yellow (82), or Spectrum Yellow (79). Ventral coloration of paratypes generally falls into two categories: individuals with venters similar to those of the holotype, featuring a gray to purple coloration with purple adjacent to the ventrolateral stripe; and individuals with ventral coloration featuring pale to bright yellow in place of purple (Fig.

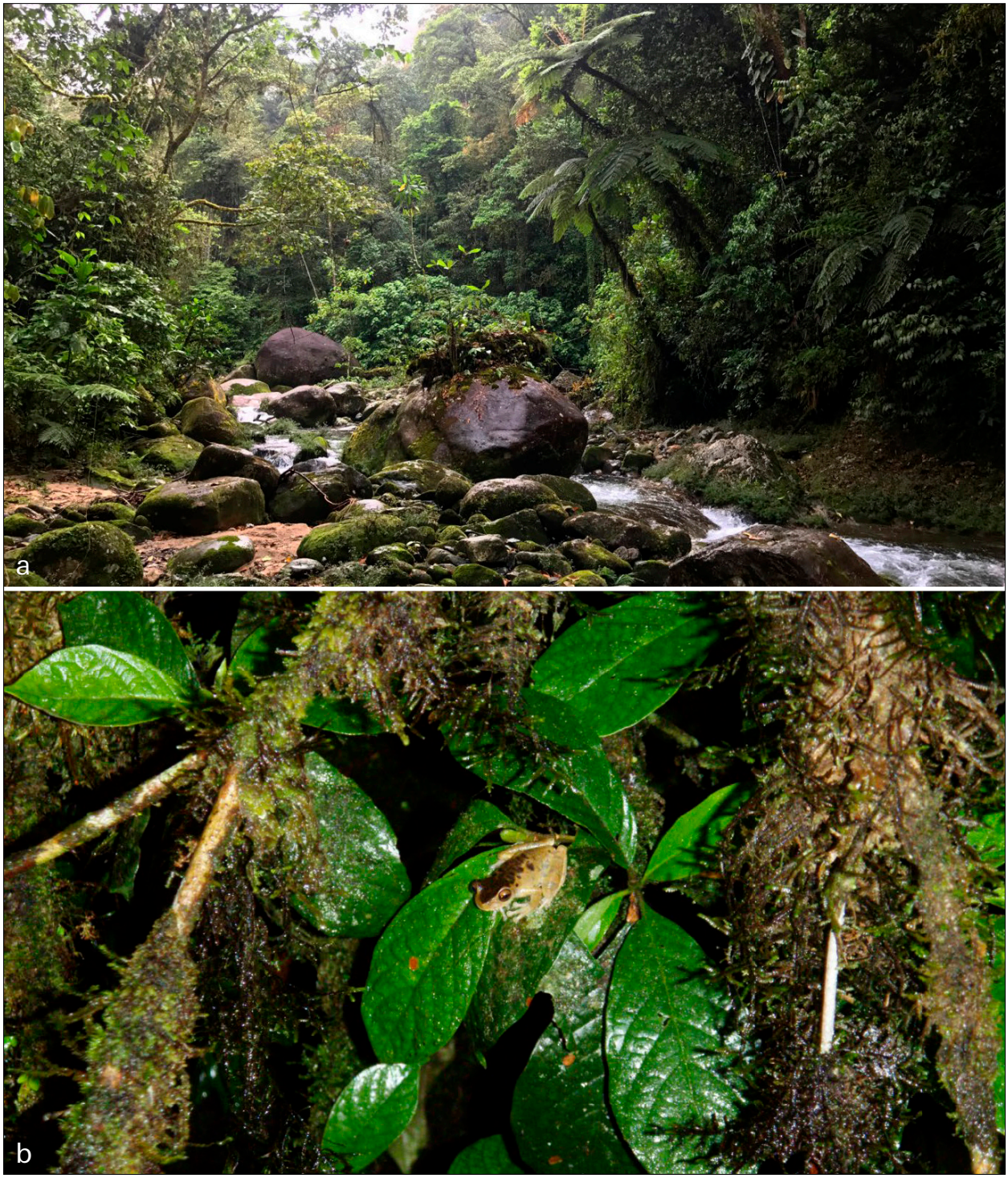

Fig. 9. a) Type locality of *Atlantihyla melissa*, the Río Jilamito, Departamento de Atlántida, Honduras, 1,030 m a.s.l.; holotype was collected on a palm frond in the vegetation on the left side of the image. **b**) Adult male *A. melissa* (not collected) photographed in situ on vegetation directly overhanging a small tributary of the Río Jilamito, 1,060 m a.s.l. (photographs © JHT).

11a). These yellow-phase individuals can have immaculate or Pale Buff venters, with ventral surfaces of front and hindlimbs being Pale Greenish Yellow (86), Sulphur Yellow (80), Spectrum Yellow (79), or Dark Spectrum Yellow (78). The chin and throats of most individuals are immaculate; however, occasional individuals have dark spots that can be scattered or make the chin appear mottled.

Description of tadpole. A tadpole (CM 163366; Fig. 13A) from the type locality, exhibiting Gosner (1960) development stage 36, is described as follows: TL 43.5 mm, BL 13.5 mm, BW 7.1 mm, EL 1.4 mm, IOD 4.1 mm, IND, TAL 30.1, TMH 4.7 mm, TMW 3.6 mm; body somewhat compressed, wider than high; snout broad and rounded in dorsal aspect, rounded in lateral view; eyes positioned dorsolaterally, EL/BL 0.104; nostrils small,

directed anteriolaterally, and positioned slightly closer to eyes than tip of snout; spiracle single, sinistral, directed posteriorly, opening on midline of body approximately two-thirds distance from tip of snout to posterior end of body; vent tube short, dextral; hind limb buds with separation between toes II–III, III–IV, and IV–V; tail more than twice length of body, TAL/TL 0.692; tail musculature not extending to tip of tail, tail fins relatively shallow, tail musculature at midlength of tail slightly taller than height of dorsal or ventral tail fins at same point; oral disk large (Fig. 13b), ventral, with continuous border of 2–3 rows of marginal papillae, with 4–5 rows of submarginal papillae present at level lateral to jaw sheath; labial tooth rows 5–6/8–9, appearing somewhat irregular with most rows exhibiting some degree of interruption or fragmentation: row A-1 with four narrow interruptions, row A-2 with one narrow lateral interruption, A-3 with two narrow lateral interruptions, A-4 with two narrow and one wide lateral interruptions, A-5 broadly interrupted by A-6, which shift anteriorly to take position of A-5 while A-5 reappears medially in position of A-6, P-1 with one narrow medial and one narrow lateral interruption, P-4 with one narrow lateral interruption, P-5 appearing as a partial row about one-fifth length of P-4, P-7 with two lateral interruptions, P-8 and P-9 highly fragmented (Fig. 13b). Coloration in preservative: body mottled grayish-tan, tail musculature pale tan with brown blotches; tail fins translucent with scattered dark flecking and a few dark spots on the anterior portion of the dorsal fin.

Advertisement call. The advertisement call of an adult male (UVS V671) from the type locality consists of a series of 5–6 relatively long pulsed notes, presented in a continuous or nearly continuous call series, which increases in amplitude with each note and the final note of each call being the strongest; sometimes followed by a single faint trailing note that can lead into the next call (Fig. 6a). Spectrum visualization revealed two harmonics present in each note (Fig. 6). Dominant frequency of the entire call series was 3421.9 Hz. Calls had the following quantitative spectral and temporal characteristics (n = 4): call duration 8.28–13.19 s (n = 4, x = 11.16 ± 2.15), 5–6 (x = 5.25 ± 0.5) notes per call, note duration 0.47–1.3 s (n = 16, x = 0.913 ± 0.21), note repetition rate 0.405–0.604 calls/s (x = 0.481 ± 0.09), interval between notes 1.04–1.79 s (n = 14, x = 1.466 ± 0.211), 5–12 (x = 8.21 ± 2.16) pulses per note, pulse duration 0.013–0.052 s (n = 153, x = 0.027 ± 0.004), pulse repetition rate 5.669–11.086 (x = 9.359 ± 1.375), peak amplitude of each pulse 287–2982 U (x = 1288.29 ± 644.22), inter-pulse interval 0.035–0.106 s (n = 134, x = 0.074 ± 0.008).

Etymology. We name this species in honor of our friend and collaborator, Isis Melissa Medina-Flores, a field biologist originally from Mangulile in the Department of Olancho, Honduras. Melissa participated in the discovery and description of this new species, two other Texiguat endemics: the palm-pitviper *Bothriechis guifarroi* Townsend, Medina-Flores, Wilson, Jadin & Austin, 2013, and the centipede snake *Tantilla olympia* Townsend, Wilson, Medina-Flores & Herrera-B., 2013; and two salamanders endemic to the Department of Olancho: *Nototriton mime* Townsend, Medina-Flores, Reyes-Calderón & Austin, 2013, and *N. picucha* Townsend, Medina-Flores, Murillo, and Austin, 2011. Melissa disappeared without a trace on 5 November 2016, after becoming separated from her companions while descending from the summit of the highest peak in Honduras, Cerro de Las Minas in Parque Nacional Celaque. Despite over a month of continuous searching by military and volunteer rescue teams supported by search dogs and aircraft, no evidence of Melissa's fate has been found.

Distribution. This species is known to occur between 780–1,680 m elevation in the western portion of the Cordillera Nombre de Dios, Departments of Atlántida and Yoro, Honduras, from localities nearly completely contained within the boundaries of Refugio de Vida Silvestre Texiguat. The distribution of *A. melissa* appears to be centered on the Río Jilamito Valley, where the majority of remaining habitat exists, and extends to the south across the ridge and peaks associated with Cerro Texiguat and into broadleaf riparian zones on the leeward slopes of those peaks.

Natural history. *Atlantihyla melissa* is found in intact Broadleaf Transitional Cloud Forest and peripherally in Broadleaf Cloud Forest (Townsend, 2014), corresponding to the Premontane Wet Forest formation and Lower Montane Wet Forest formations, respectively, of Holdridge (1967). This species occurs in association with fast-flowing rivers and streams with rocky substrates, a mix of pools and riffles, and abundant riparian vegetation (Figs. 9, 10). The locality in the Department of Yoro on the leeward side of RVS Texiguat (Fig. 10d–e) consists of a stream and associated broadleaf riparian vegetation flowing through a series of ravines, otherwise surrounded by *Ocotal* (pine-oak forest) and Mixed Transitional Cloud Forest habitat (Townsend, 2014). Individuals were commonly encountered at night on vegetation near or overhanging the water (Figs. 9b, 12). Males were actively vocalizing in March and April, including intermittently from concealed positions during daytime, with vocalizations also being present, but more intermittent, during June and July. Females observed during March had well-developed eggs visible in their oviducts. Emerging and recently emerged metamorphs (Figs. 13c, 13d) were abundant in June and July on rocks and low vegetation adjacent to the Río Jilamito and tributaries, while tadpoles were abundant in pools.

At premontane elevations (780–1,430 m) in the vicinity of the Río Jilamito and its tributaries, *A. melissa* is part of a community of stream-associated anurans that includes the endemic treefrogs *Duellmanohyla salvavida* and *Plectrohyla chrysopleura*, the endemic streamside frog *Craugastor aurilegulus*, and the glassfrog *Teratohyla pulverata*. Townsend *et al*. (2012: 100) provided a

Fig. 10. Habitat of *A. melissa*: (**a**) Large pool in the Río Jilamito, just above the type locality; tadpoles of *A. melissa*. *Duellmanohyla salvavida*, and *Plectrohyla chrysopleura* were found here in April 2017, June 2010, and July 2010. (**b**) Small tributary of the Río Jilamito above the type locality, 1,090 m a.s.l., adults and tadpoles of *A. melissa* and *D. salvavida* were abundant here in June and July 2010. (**c**) Small tributary of the Río Jilamito directly adjacent to the type locality, 1,060 m a.s.l. adults, metamorphs, and tadpoles of *A. melissa*, *D. salvavida,* and *P. chrysopleura* were abundant here in June and July 2010. (**d**) Stream habitat approximately 2.5 airline km north-northeast of La Fortuna, Departamento de Yoro, where *A. melissa* has been collected alongside endemic anurans *Craugastor saltuarius*, *C. stadelmani*, *D. salvavida*, *Isthmohyla insolita*, and *Plectrohyla cf. guatemalensis*, (**e**) Same stream as 10(d) showing extensive deforestation approximately 200 m upstream in April 2008 (photographs © JHT).

detailed overview of the herpetofaunal community present at the type locality of *A. melissa*, describing populations of this species as "extremely abundant" and the "most commonly encountered amphibian" around the Río Jilamito and its tributaries at the site known as La Liberacíon. At higher elevations (1,550–1,680 m) on the leeward slopes of RVS Texiguat, *A. melissa* is found in sympatry with the endemic stream-associated treefrogs

Fig. 11. Paratypes of *Atlantihyla melissa* in life: (**a**) adult female (USNM 578676), (**b**) adult female (USNM 578672), (**c**) adult female (USNM 578665), (**d**) adult female (USNM 578686), (**e**) adult male (USNM 578674), (**f**) adult female (USNM 578668) (photographs © JHT).

D. salvavida, *Isthmohyla insolita*, and *Plectrohyla cf. guatemalensis*, and also been documented in near-sympatry with *Atelophryniscus chrysophorus*, *C. saltuarius*, and *C. stadelmani*, three species of terrestrial streamside anurans also considered endemic to the Cordillera Nombre de Dios (McCranie & Wilson, 2002).

Conservation status. Prior to this study, *Atlantihyla spinipollex sensu lato* was considered Endangered (B1ab[iii] + 2ab[iii]) on the IUCN Red List due to loss of habitat from subsistence agriculture and land-clearing for timber and pastureland (Cruz *et al*., 2004). Application of the IUCN Red List criteria (IUCN 2012; IUCN Standards and Petitions Committee, 2019) indicates that *A. spinipollex sensu stricto* should remain Endangered (B1ab[iii]+2ab[iii]), and that *A. melissa* should be considered Critically Endangered (B1ab[iii]) due to the known distribution being limited to a single threat-defined area of highland forest < 25 km^2 in total extent, which is undergoing a continuous decline in the extent and quality of remaining habitat due to ongoing deforestation and development.

Remarks. Köhler (2011: 258–259) included photographs of the holotype and two paratypes (USNM 578664, 578662) as *P.* (= *A.*) *spinipollex*, and Townsend *et al*. (2012: 101) also provided photographs of the holotype, and one paratype (USNM 578686), and one un-

Fig. 12. Variation in color pattern among unvouchered *Atlantihyla melissa* photographed in situ at night along the Río Jilamito and associated tributaries at the type locality (1,030–1,090 m a.s.l.; photographs © JHT).

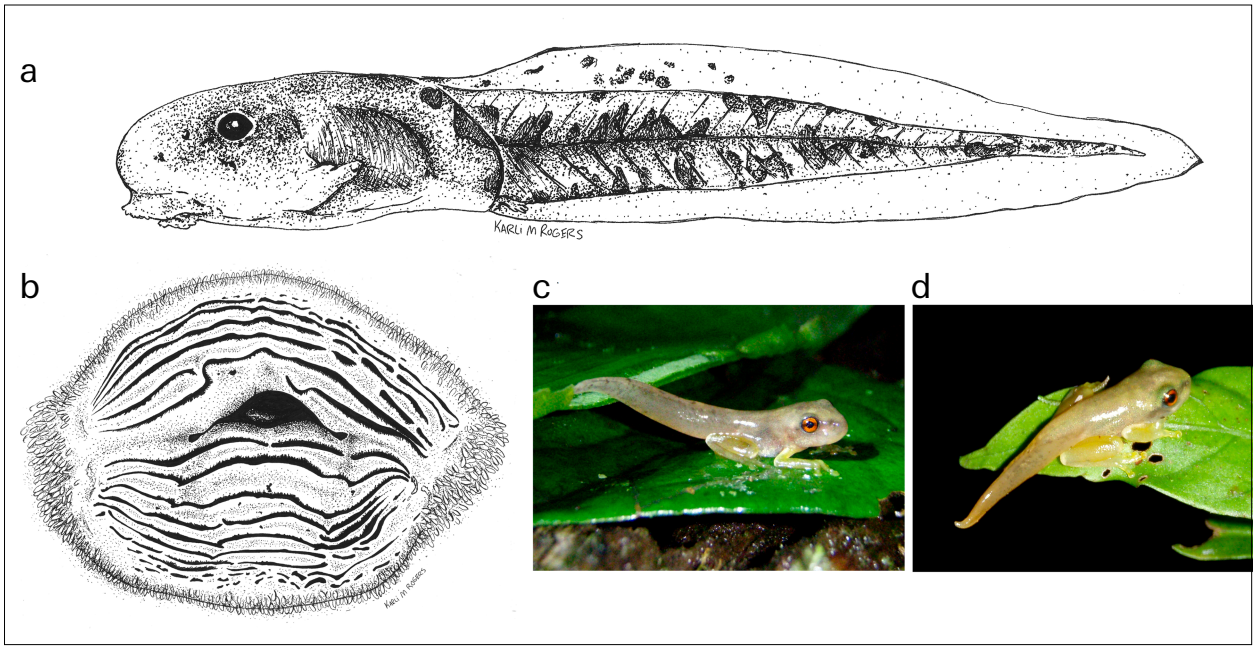

Fig. 13. Semi-diagrammatical illustrations of the (**a**) larva of *Atlantihyla melissa* (CM 163366; Gosner stage 36, TL = 43.5 mm) and (**b**) oral disk of the same larva, and images of two recently emerged metamorphs (not collected) of *A. melissa* (**c, d**) photographed in situ at the type locality (photographs © JHT).

vouchered individual (Fig. 12j) as *P*. (= *A*.) *spinipollex*, but incorrectly labeled the holotype as an adult female (rather than male) in Fig. 5d. The lowest recorded elevation for *A*. *melissa* (780 m) is based on an unvouchered individual encountered by JHT at a point where the trail to La Liberación crossed a tributary of the Río Jilamito on 13 March 2017.

Discussion

Biogeography and taxonomy of stream treefrogs in the Chortís Highlands

The three species of *Atlantihyla*— *A*. *melissa*, *A*. *panchoi*, and *A*. *spinipollex*—are distributed across three highland areas on the Caribbean slope of Nuclear Central America. The distribution of these species is notable in that the genus appears to be absent from the intervening highlands of the Sierra de Omoa and Sierra de Espíritu Santo, highlands that otherwise support a rich endemic herpetofauna. While the cause for the absence of *Atlantihyla* spp. from the highlands of the Guatemala-Honduras border area is unclear, this pattern of distribution may be a reflection of the historical ecophysiography and geology of the Chortís Block, which hypothetically would have placed the contemporary Cordillera Nombre de Dios adjacent to the highlands containing the modern distribution of *A*. *panchoi* during the early Miocene (Townsend, 2014). A similar pattern of potential "tectonic rafting" in relation to Chortís Block endemics and their Maya Block relatives may also be demonstrated in the salamander genus *Dendrotriton* (Rovito *et al*., 2012), although hypotheses related to this phenomenon have not been explicitly tested and the history of geological movement of the Chortís Block remains a matter of some debate.

Questions remain concerning the deeper evolutionary history and taxonomy of certain stream treefrog populations both within and extralimital to the Chortís Highlands. The application of large, multilocus datasets to such questions has resolved many species-level relationships within Hylini (Campbell *et al*., 2018; Caviedes-Solis & Nieto-Montes de Oca, 2018; Duellman *et al*., 2016; Faivovich *et al*., 2005, 2018), greatly improving our understanding of the species within this tribe. However, deeper relationships between and within some genera remain uncertain and without satisfactory resolution. Challenging groups, such as *Duellmanohyla* and *Sarcohyla*, continue to present problems particularly when molecular and morphological evidence infer contradictory results. These lineages might have previously experienced evolutionary processes—such as reticulate evolution or introgression—that are not detectable without genomic scale datasets and which result in confusing morphological overlap (Burbrink & Gehara, 2018; Grummer *et al*., 2018; Morales-Briones *et al*., 2018; Firneno *et al*., 2020). Clearly, improved genomic sampling, together with more robust hypothesis testing, are needed to better understand the complex evolutionary history of these taxa.

Patterns of diversification in *Ptychohyla hypomykter*

In the first comprehensive review of the genus *Ptychohyla*, Duellman (1963: 330) noted that specimens of *P*. (=*Atlantihyla*) *spinipollex* from Honduras, including the holotype, differed from populations in Guatemala in ventral coloration, and Duellman (1970: 547) reiterated observations of distinctiveness between samples from Honduras and those from Guatemala, suggesting that they eventually might be found to represent distinct taxa. While these observations were confounded by the confusion at that time between *A*. *spinipollex* and populations later described as *P*. *hypomykter* (McCranie & Wilson, 1993), Faivovich *et al*. (2018) found samples representing *P*. *hypomykter sensu stricto* from Honduras were widely paraphyletic with respect to two available samples from Guatemala (UTA A-51040 and UTA A-51088) and appeared to represent a distinct taxon (Duellman *et al*., 2016; Faivovich *et al*., 2005, 2018). Our results provide further support for the distinctiveness of the central Guatemala samples, and we recovered a well-supported, reciprocally monophyletic *Ptychohyla hypomykter sensu stricto* clade that included a sample of *P*. *hypomykter* (JHT 2855) from the type locality and 55 samples from 20 other localities across the Chortís Block sequenced for 16S (Figs. 1–3). The central Guatemala samples are from localities to the west and north of the Motagua-Polochic Fault system, previously recognized as a biogeographic barrier for highland amphibians and reptiles (Castoe *et al*., 2009; Hofmann & Townsend, 2017; Jadin *et al*., 2012; Rovito & Parra-Olea, 2016).

Within *Ptychohyla hypomykter sensu stricto*, our analysis of 56 samples using the mitochondrial locus 16S recovered three geographically distinct haplotype groups (Figs. 1, 2). The "western" haplogroup was represented by five samples from the Sierra de Omoa, Sierra de Espíritu Santo, Sierra de Joconal, and Sierra de Merendón in the departments of Copán, Cortés, Ocotepeque, and Santa Bárbara in western Honduras, and included localities along the border with Guatemala. The "central" haplogroup includes 32 samples from Montaña de Meámbar, Montaña de Santa Bárbara, Sierra de Comayagua, and Sierra de Sulaco in central Honduras, while the "eastern-southern" haplogroup includes 19 samples from the Montaña de Jacaleapa and Sierra de Botaderos in the Department of Olancho in northwestern Honduras and the Cordillera Dariense in the departments of Jinotega and Matagalpa, Nicaragua. Given this structure and relative lack of diversification (albeit based on a single, relatively conserved mtDNA fragment) across at least 14 isolated highland areas (Fig. 1)—many of which support their own endemic species—we hypothesize that *P*. *hypomyk-*

ter underwent a relatively recent expansion across the Chortís Block, possibly following the last glacial maximum when isolation among highland areas might have been reduced. While our results provide some initial insight into intraregional patterns of diversification in the Chortís Block, fine-scale analysis of phylogeographic patterns, supplemented with data from more variable loci, is needed to better elucidate patterns and timing of recent diversification within *P. hypomykter*.

Habitat loss and continuing threats to Refugio de Vida Silvestre Texiguat

The importance of Refugio de Vida Silvestre Texiguat as a hotspot for biological endemism, and the continually expanding threats to that endemism, have been well-documented over the past three decades (Holm & Cruz, 1994; McCranie & Castañeda, 2004a, b; McCranie *et al*., 1993; Townsend *et al*., 2012; Wilson *et al*., 1998). At least 12 site-restricted endemic species of amphibians and reptiles are known only from the environs of RVS Texiguat. The Río Jilamito and its tributaries in the vicinity of La Liberación are also home to the only known extant population of the Critically Endangered spikethumb treefrog *Plectrohyla chrysopleura*, which was discovered there in 2010 after being feared extinct (Townsend *et al*., 2011). The reserve also protects habitat for at least 14 additional herpetofaunal species that are otherwise endemic to Honduras (McCranie, 2018; Townsend *et al*., 2012; Townsend *et al*., 2013a), giving RVS Texiguat the unique opportunity to conserve no fewer than 27 species of endemic amphibians and reptiles and stand as a veritable "crown jewel" of endemic biodiversity in Honduras and the whole of Mesoamerica.

Despite the strong base of scientific data supporting the value of RVS Texiguat, particularly the Jilamito Valley that forms the heart of the reserve, destruction and exploitation of the remaining forest appears to be continuing apace. Illegal extraction of timber, and subsequent illegal land-clearing for coffee farms and livestock have historically been the primary causes of forest loss within the reserve's boundaries. Additionally, development has begun on a project to build a 14-megawatt hydroelectric dam on the Río Jilamito at the La Liberación site, just outside the legal boundary of the nuclear zone at the type localities of *Atlantihyla melissa*, the salamander *Nototriton nelsoni* (Townsend, 2016), the centipede snake *Tantilla olympia* (Townsend *et al*., 2013a), and the palm-pitviper *Bothriechis guifarroi* (Townsend *et al*., 2013b). This project comes as the steady expansion of deforestation on the southwestern, southern, and eastern edges of RVS Texiguat has begun to reach into the heart of the reserve, with the first patches of deforestation appearing in 2014 in the previously undisturbed upper Jilamito Valley. Without an immediate, sustained, and verifiable effort to protect the remaining forests of RVS Texiguat, there can be little doubt that habitat loss will continue until what remains has lost its ecological functionality and associated endemic community. To paraphrase Edward O. Wilson (Sheppard, 1990), the loss of such a unique biological community in the name of short-term economic gains would be akin to burning a Renaissance painting to cook a meal. The biological diversity we stand to lose in the Río Jilamito Valley cannot be replaced or mitigated, as they exist nowhere else on earth, and our window of opportunity to conserve these unique resources for the next generation is rapidly closing.

Acknowledgments

We are indebted to the following individuals and organizations for supporting our work in Refugio de Vida Silvestre Texiguat in 2010: Allan J. Fuentes (PROLANSATE); Adolfo Pagoada-Saybe (Municipalidad de Arizona), Saíd Laínez, Iris Acosta, Roberto Downing, Andrés Alegría (ICF); *guardabosques* Efrain Aguilar (San José de Texiguat), Arnaldo Contreras (Mezapita), and Alionso Portillo (Jilamito Nuevo); and José "Juan" Arita, *majordomo* at La Liberación. We thank Benjamin K. Atkinson, César A. Cerrato, Levi N. Gray, Paul House, Mayron McKewy Mejía, Ciro Navarro-Umaña, Alexander L. Stubbs, and Hermes Vega-Rodríguez for their valued assistance and hard work in the field. We are also grateful to Javier Sunyer and Scott L. Travers for providing some samples for comparative genetic analysis. Fieldwork was supported in part by grants to JHT from the Critical Ecosystem Partnership Fund, the Indiana University of Pennsylvania (IUP) Department of Biology, IUP College of Natural Sciences and Mathematics, IUP School of Graduate Studies and Research, IUP Faculty Senate, Commonwealth of Pennsylvania University Biologists (CPUB), and a Pennsylvania State System of Higher Education Faculty Professional Development Grant. Amy Driskell and Dan Mulcahy (Smithsonian Institution Laboratory of Analytical Biology) contributed some of the raw 16S sequence data, in collaboration with Roy McDiarmid (USNM) as part of the "Barcoding the Herpetofauna of Eastern Nuclear Central America" project. We thank Roy McDiarmid, Jeremy Jacobs, Steve Gotte, and John Poindexter (USNM) for facilitating and preparing the loan of comparative materials and accessioning the type series, and Steve Rogers, Jennifer Sheridan, Stevie Kennedy-Gold, and Kaylin Martin (CM) for accessioning the tadpole used to prepare Figure 13 and some comparative specimens. Esbeiry Cordova-Ortiz and T.J. Firneno, Jr. provided additional assistance in obtaining molecular data in the laboratory. Finally, our paper was greatly improved by the artistic contributions of Karli Rogers, who provided hand, foot, tadpole, and oral disk illustrations. This manuscript and revisions were completed while JHT was a Fulbright Scholar and Visiting Professor at the Centro Zamorano de Biodiversidad, and JHT would like to thank Narayanaswamy Bharathan, Deanne Snavely, Timothy Moerland, Erika Tenorio, Oliver Komar, and Eric Van De Berghe for their support.

References

Bioacoustics Research Program. (2014). *Raven Pro: Interactive Sound Analysis Software* (*Version 1.5*) [Computer software]. Ithaca, NY: The Cornell Lab of Ornithology. Retrieved from http://www.birds.cornell.edu/raven

Bossuyt, F. & Milinkovitch, M. C. (2000). Convergent adaptive radiations in Madagascan and Asian ranid frogs reveal covariation between larval and adult traits. *Proceedings of the National Academy of Sciences USA*, **97**, 6585–6590.

Bouckaert, R., Heled, J., Kühnert, D., Vaughan, T., Wu, C-H., Xie, D., Suchard, Ma., Rambaut, A. & Drummond, A. J. (2014). beast 2: A software platform for Bayesian evolutionary analysis. *PLoS Computational Biology*, **10**, e1003537.

Burbrink, F. T. & Gehara, M. (2018). The biogeography of deep time phylogenetic reticulation. *Systematic Biology*, **67**, 743–755.

Campbell, J. A., Brodie Jr., E. D., Caviedes-Solis, I. W., Nieto-Montes de Oca, A., Luja, V. H., Flores-Villela, O., García-Vázquez, U. O., Sarker, G. C., Wostl, E. & Smith, E. N. (2018). Systematics of the frogs allocated to *Sarcohyla bistincta* sensu lato (Cope, 1877), with description of a new species from Western Mexico. *Zootaxa*, **4422**, 366–384.

Castoe, T. A., Daza, J. M., Smith, E. N., Sasa, M. M., Kuch, U., Campbell, J. A., Chippindale, P. T. & Parkinson, C. L. (2009). Comparative phylogeography of pitvipers suggests a consensus of ancient Middle American highland biogeography. *Journal of Biogeography*, **36**, 88–103.

Caviedes-Solis, I. W. & Nieto-Montes de Oca A. (2018). A multilocus phylogeny of the genus *Sarcohyla* (Anura: Hylidae), and an investigation of species boundaries using statistical species delimitation. *Molecular Phylogenetics and Evolution*, **118**, 184–193.

Crawford, A. J. & Smith, E. N. (2005). Cenozoic biogeography and evolution in direct-developing frogs of Central America (Leptodactylidae: *Eleutherodactylus*) as inferred from a phylogenetic analysis of nuclear and mitochondrial genes. *Molecular Phylogenetics and Evolution*, **35**, 536–555.

Cruz, G., Wilson, L. D. & McCranie, J. R. (2004) *Ptychohyla spinipollex*. *The IUCN Red List of Threatened Species*, **2004**, e.T55918A11391648.

Duellman, W. E. (1963). A review of the Middle American treefrogs of the genus *Ptychohyla*. *University of Kansas Publications*, *Museum of Natural History*, **15**, 297–349.

Duellman, W. E. (1970). *The Hylid Frogs of Middle America*. Lawrence, KS, Museum of Natural History, University of Kansas.

Duellman, W. E. (2001) *Hylid Frogs of Middle America* (2nd ed.). Ithaca, New York, Society for the Study of Amphibians and Reptiles.

Duellman, W. E., Marion, A. B. & Hedges, S. B. (2016). Phylogenetics, classification, and biogeography of the treefrogs (Amphibia: Anura: Arboranae). *Zootaxa*, **4104**, 1–109.

Faivovich, J., Haddad, C. F. B., García, P. C. A., Frost, D. R., Campbell, J. A. & Wheeler, W. C. (2005). Systematic review of the frog family Hylidae, with special reference to Hylinae: phylogenetic analysis and taxonomic revision. *Bulletin of the American Museum of Natural History*, **294**, 1–240.

Faivovich, J., Pereyra, M. O., Luna, M. C., Hertz, A., Blotto, B. L., Vásquez-Almazán, C. R., McCranie, J. R., Sánchez, D. A., Baêta, D., Araujo-Vieira, K., Köhler, G., Kubicki, B., Campbell, J. A., Frost, D. R., Wheeler, W. C. & Haddad, C. F. B. (2018). On the monophyly and relationships of several genera of Hylini (Anura: Hylidae: Hylinae), with comments on recent taxonomic changes in hylids. *South American Journal of Herpetology*, **13**, 1–32.

Firneno, Jr., T. J., J. R. O'Neill, D. M. Portik, A. H. Emery, J. H. Townsend & M. K. Fujita. (2020). Finding complexity in complexes: assessing the causes of mitonuclear discordance in a problematic species complex of Mesoamerican toads. *Molecular Ecology*, **29**, 3543–3559.

Fujisawa, T. & Barraclough, T. G. (2013). Delimiting species using single-locus data and the generalized mixed yule coalescent approach: a revised method and evaluation on simulated data sets. *Systematic Biology*, **62**, 702–724.

Goebel, A. M., Donnelly, J. M. & Atz, M.E. (1999). PCR primers and amplification methods for 12S ribosomal DNA, the control region, cytochrome oxidase I, and cytochrome b in Bufonids and other frogs, and an overview of PCR primers which have amplified DNA in amphibians successfully. *Molecular Phylogenetics and Evolution*, **11**, 163–199.

Gosner, K. L. (1960). A simplified table for staging Anuran embryos and larvae with notes on identification. *Herpetologica*, **16**, 183–190.

Grummer, J. A., Morando, M. M., Avila, L. J., Sites Jr., J. W. & Leaché, A. D. (2018). Phylogenomic evidence for a recent and rapid radiation of lizards in the Patagonian *Liolaemus fitzingerii* species group. *Molecular Phylogenetics and Evolution*, **125**, 243–254.

Gutiérrez-García, T. A. & Vásquez-Domínguez, E. (2013). Consensus between genes and stones in the biogeographic and evolutionary history of Central America. *Quaternary Research*, **79**, 311–324.

Hofmann, E. P. & Townsend, J. H. (2017). Origins and biogeography of the *Anolis crassulus* subgroup (Squamata: Dactyloidae) in the highlands of Nuclear Central America. *BMC Evolutionary Biology*, **17**, 267.

Holdridge, L. R. (1967). *Life Zone Ecology* (Revised ed.). San José, Costa Rica, Tropical Science Center.

Huelsenbeck, J. P. & Ronquist, F. (2001). mrbayes: Bayesian inference of phylogenetic trees. *Bioinformatics*, **17**, 754–755.

IUCN (2012) *IUCN Red List Categories and Criteria: Version 3.1*. *Second Edition*. Gland, Switzerland and Cambridge, United Kingdom, IUCN.

IUCN Standards and Petitions Committee. (2019). *Guidelines for Using the IUCN Red List Categories and Criteria*. *Version 14*. Prepared by the Standards and Petitions Committee. Downloaded 23 Feb 2020 from http://www.iucnredlist.org/documents/RedListGuidelines.pdf.

Jadin, R. C., Townsend, J. H., Castoe, T. A. & Campbell, J. A. (2012). Cryptic diversity in disjunct populations of Middle American montane pitvipers: a systematic reassessment of *Cerrophidion godmani*. *Zoologica Scripta*, **41**, 455–470.

Jordan, B. R., Sigurdsson, H. & Carey, S. N. (2008). *Ignimbrites in Central America and Associated Caribbean Sea Tephra: Correlation and Petrogenesis*. Saarbrücken, VDM Verlag.

Köhler, G. (2011). *Amphibians of Central America*. Offenbach, Herpeton.

Köhler, G. (2012). *Color Catalogue for Field Biologists*. Offenbach, Herpeton.

Köhler, J., Jansen, M., Rodríguez, A., Kok, P. J. R., Toledo, L. F., Emmrich, M., Glaw, F., Haddad, C. F. B., Rödel, M. O. & Vences, M. (2017). The use of bioacoustics in anuran taxonomy: theory, terminology, methods and recommendations for best practice. *Zootaxa*, **4251**, 1–124.

Kumar, S., Stecher, G. & Tamura, K. (2016). MEGA7: Molecular evolutionary genetics analysis version 7.0 for bigger datasests. *Molecular Biology and Evolution*, **33**, 1870–1874.

Lanfear, R., Calcott, B., Ho, S. Y. & Guindon, S. (2012). Partitionfinder: combined selection of partitioning schemes and substitution models for phylogenetic analysis. *Molecular Biology and Evolution*, **29**, 1695–1701.

Luque-Montes, I., Austin, J. D., Weinfurther, K. D., Wilson, L. D., Hofmann, E. P. & Townsend, J. H. (2018). An integrative assessment of the taxonomic status of putative hybrid leopard frogs (Anura: Ranidae) from the Chortís Highlands of Central America, with description of a new species. *Systematics and Biodiversity*, **16**, 340–356.

McCranie, J. R. (2018). The lizards, crocodiles, and turtles of Honduras. Systematics, distribution, and conservation. *Bulletin of*

the Museum of Comparative Zoology, *Special Publications Series*, **2**, 1–666.

McCranie, J. R. & Castañeda, F. E. (2004a). A new species of snake of the genus *Omoadiphas* (Reptilia: Squamata: Colubridae) from the Cordillera Nombre de Dios in northern Honduras. *Proceedings of the Biological Society of Washington*, **117**, 311–316.

McCranie, J.R. & Castañeda, F. E. (2004b). Notes on the second specimens of *Geophis damiani* Wilson, McCranie, and Williams and *Rhadinella tolpanorum* Holm and Cruz D. (Colubridae). *Herpetological Review*, **35**, 341.

McCranie, J. R. & Solís, J. M. (2013). Additions to the amphibians and reptiles of Parque Nacional Pico Bonito, Honduras, with an updated nomenclatural list. *Herpetology Notes*, **6**, 239–243.

McCranie, J. R & Wilson, L. D. (1993). Taxonomic changes associated with the names *Hyla spinipollex* Schmidt and *Ptychohyla merazi* Wilson and McCranie (Anura: Hylidae). *The Southwestern Naturalist*, **38**, 100–104.

McCranie, J. R. & Wilson, L. D. (2002). *The Amphibians of Honduras*. Ithaca, NY, Society for the Study of Amphibians and Reptiles.

McCranie, J. R., Wilson, L. D. & Williams, K. L. (1993). New species of tree frog of the genus *Hyla* (Anura: Hylidae) from Northern Honduras. *Copeia*, **1993**, 1057–1062.

Morales-Briones, D. F., Romoleroux, K., Kolár, F. & Tank, D. C. (2018). Phylogeny and evolution of the neotropical radiation of *Lachemilla* (Rosaceae): Uncovering a history of reticulate evolution and implications for infrageneric classification. *Systematic Botany*, **43**, 17–34.

Palumbi, S. R., Martin, A., Romano, S., McMillan, W. O., Stice, L. & Grabowski, G. (1991) *The Simple Fool's Guide to PCR*. Honolulu, HI, Department of Zoology, University of Hawaii.

Pons, J., Barraclough, T. G., Gomez-Zurita, J., Cardoso, A., Duran, D. P., Hazell, S., *et al*. (2006). Sequence-based species delimitation for the DNA taxonomy of undescribed insects. *Systematic Biology*, **55**, 595–609.

Puillandre, N., Lambert, A., Brouillet, S. & ACHAZ, G. (2012). ABGD, Automatic Barcode Gap Discovery for primary species delimitation. *Molecular Ecology*, **21**, 1864–1877.

R Core Team (2017) *R: A language and environment for statistical computing*. Vienna, R Foundation for Statistical Computing.

Rogers, R., Karason, H. & van der Hilst, R. (2002). Epeirogenic uplift above a detached slab in northern Central America. *Geology*, **30**, 1031–1034.

Ronquist, F. & Heulsenbeck, J. P. (2003). MrBayes 3: Bayesian phylogenetic inference under mixed models. *Bioinformatics*, **19**, 1572–1574.

Rovito, S.M. & Parra-Olea, G. (2016). Neotropical plethodontid biogeography: insights from molecular phylogenetics. *Copeia*, **2016**, 222–232.

Rovito, S. M., Wake, D. B., Papenfuss, T. J., Parra-Olea, G., Muñoz-Alonso, A. & Vásquez-Almazán, C. R. (2012). Species formation and geographical range evolution in a genus of Central American cloud forest salamanders (*Dendrotriton*). *Journal of Biogeography*, **39**, 1251-1265.

Rovito, S. M., Parra-Olea, G., Recuero, E. & Wake, D. B. (2015). Diversification and biogeographical history of Neotropical plethodontid salamanders. *Zoological Journal of the Linnean Society*, **175**, 167–188.

Sabaj Peréz, M. H. (2016) *Standard symbolic codes for institutional resource collections in herpetology and ichthyology: An online reference*. Version 6.5 (16 August 2016). Washington, DC, Society of Ichthyologists and Herpetologists.

Schmidt, K. P. (1936). New amphibians and reptiles from Honduras in the Museum of Comparative Zoology. *Proceedings of the Biological Society of Washington*, **49**, 43–50.

Seutin, G., White B. N & Boag P. T. (1991) Preservation of avian blood and tissue samples for DNA analyses. *Canadian Journal of Zoology*, **69**, 82–90.

Sheppard, R. Z. (1990). Nature: Splendor in the grass. Time Magazine, 3 September 1990 (retrieved 18 October 2018: http://content.time.com/time/magazine/article/0,9171,971049,00.html).

Stamatakis, A. (2014). RAxML version 8: a tool for phylogenetic analysis and post-analysis of large phylogenies. *Bioinformatics*, **30**, 1312–1313.

Stuart, L. C. (1943). Comments on the herpetofauna of the Sierra de los Cuchumatanes of Guatemala. *Occasional Papers of the Museum of Zoology*, *University of Michigan*, **471**, 1–28.

Stuart, L. C. (1948). The amphibians and reptiles of Alta Verapaz Guatemala. *Miscellaneous Publications of the Museum of Zoology*, *University of Michigan*, **69**, 1–109.

Stuart, L. C. (1954). Descriptions of some new amphibians and reptiles from Guatemala. *Proceedings of the Biological Society of Washington*, **67**, 159–178.

Tang, Y., Horikoshi, M. & Li, W. (2016). ggfortify: Unified interface to visualize statistical results of popular R packages. *The R Journal*, **8**, 474–485.

Thompson, J. D., Higgins, D. G. & Gibson, T. J. (1994). clustal W: improving the sensitivity of progressive multiple sequence alignment through sequence weighting, position-specific gap penalties and weight matrix choice. *Nucleic Acids Research*, **22**, 4673–4680.

Townsend, J. H. (2014). Characterizing the Chortís Block biogeographic province: geological, physiographic, and ecological associations and herpetofaunal diversity. *Mesoamerican Herpetology*, **1**, 204–251.

Townsend, J. H. (2016). Taxonomic revision of *Nototriton barbouri* (Schmidt)(Caudata: Plethodontidae), with description of two new species of moss salamanders from the Cordillera Nombre de Dios, Honduras. *Zootaxa*, **4196**, 511–528.

Townsend, J. H. & Wilson, L. D. (2016). Amphibians of the Cordillera Nombre de Dios, Honduras: COI barcoding suggests underestimated taxonomic diversity in a threatened endemic fauna. *Mesoamerican Herpetology*, **3**, 910–928.

Townsend, J. H., Wilson, L. D., Cerrato M., C. A., Atkinson, B. K., Herrera-B., L. A. & Mejía, M. M. (2011). Discovery of the critically endangered treefrog *Plectrohyla chrysopleura* in Refugio de Vida Silvestre Texiguat, Honduras. *Herpetological Bulletin*, **115**, 22–25.

Townsend, J. H., Wilson, L. D., Medina-Flores, M., Aguilar-Urbina, E., Atkinson, B. K., Cerrato-Mendoza, C. A., Contreras-Castro, A., Gray, L. N., Herrera-B., L. A., Luque-Montes, I. R., McKewy-Mejía, M., Portillo-Avilez, A., Stubbs, A. L. & Austin, J. D. (2012). A premontane hotspot for herpetological endemism on the windward side of Refugio de Vida Silvestre Texiguat, Honduras. *Salamandra*, **48**, 92–114.

Townsend, J. H., L. D. Wilson, M. Medina-Flores & L. A. Herrera-B. (2013a). A new species of centipede snake in the *Tantilla taeniata* group (Squamata: Colubridae) from premontane forest in Refugio de Vida Silvestre Texíguat, Honduras. *Journal of Herpetology* **47**, 191–200.

Townsend, J. H., Medina-Flores, M., Wilson, L. D., Jadin, R. C. & Austin, J. D. (2013b). A relict lineage of green palm-pitviper (Squamata: Viperidae: *Bothriechis*) from the Chortís Highlands of Mesoamerica. *ZooKeys*, **298**, 77–105.

Wickham, H. (2016) *ggplot2: Elegant graphics for data analysis*. New York, NY, Springer.

Wiens, J. J., Fetzner Jr, J. W., Parkinson, C. L. & Reeder, T. W. (2005). Hylid frog phylogeny and sampling strategies for speciose clades. *Systematic Biology*, **54**, 778–807.

Wiens, J. J., Kuczynski, C. A., Hua, X. & Moen, D. S. (2010). An expanded phylogeny of treefrogs (Hylidae) based on nuclear and mitochondrial sequence data. *Molecular Phylogenetics and Evolution*, **55**, 871–882.

Williams, S. T. (2007). Safe and legal shipment of tissue samples: Does it affect DNA quality? *Journal of Molluscan Studies*, **73**, 416–418.

Wilson, L. D. & McCranie, J. R. (1989). A new species of *Ptychohyla* of the *euthysanota* group from Honduras, with comments on the status of the genus *Ptychohyla* Taylor (Anura: Hylidae). *Herpetologica*, **45**, 10–17.

Wilson, L.D., McCranie, J. R. & Williams, K. L. (1998). A new species of *Geophis* of the *sieboldi* group (Reptilia: Serpentes: Colubridae) from northern Honduras. *Proceedings of the Biological Society of Washington*, **111**, 410–417.

ZooBank Registration

at http://zoobank.org

This published work and the nomenclatural acts it contains have been registered in ZooBank, the online registration system for the International Commission on Zoological Nomenclature (ICZN). The ZooBank LSID (Life Science Identifier) can be resolved and the associated information can be viewed through any standard web browser by appending the LSID to the prefix http://zoobank.org. The LSID for this publication is as follows:

urn:lsid:zoobank.org:pub:21E62F29-A8A1-40DD-B96A-CE1049A05D79

Appendix 1. Taxa, museum voucher or sample ID numbers, and associated GenBank accession numbers for samples used in phylogenetic analyses; accession numbers MK176937 – 177076 and MW177722 – 177747 represent novel sequences presented in this study.

Taxon	Field ID	Museum ID	POMC	RHO	RAG1	12S	16S
A. melissa	JHT3041	USNM 578665	—	—	—	—	MK177009
A. melissa	JHT3042	USNM 578666	—	—	—	—	MK177010
A. melissa	JHT3055	USNM 578667	—	—	—	—	MK177011
A. melissa	JHT3056	USNM 578668	—	—	—	—	MK177012
A. melissa	JHT3057	USNM 578669	—	—	—	—	MK177013
A. melissa	JHT3058	USNM 578670	—	—	—	—	MK177014
A. melissa	JHT3059	USNM 578671	—	—	—	—	MK177015
A. melissa	JHT3070	USNM 578672	—	—	—	—	MK177016
A. melissa	JHT3071	USNM 578673	—	—	—	—	MK177017
A. melissa	JHT3072	USNM 578674	—	—	—	—	MK177018
A. melissa	JHT3073	USNM 578675	—	—	—	—	MK177019
A. melissa	JHT3078	—	—	—	—	—	MK177020
A. melissa	JHT3111	USNM 578651	—	—	—	—	MK177021
A. melissa	JHT3113	USNM 578653	—	—	—	—	MK177022
A. melissa	JHT3114	USNM 578679	MK177061	MK177068	MW177730	MK176937	MK176946
A. melissa	JHT3115	USNM 578680	—	—	—	—	MK177023
A. melissa	JHT3116	USNM 578681	MW177743	MW177726	MW177731	MW177722	MK177024
A. melissa	JHT3233	USNM 578685	—	—	—	—	MK177027
A. melissa	JHT3234	USNM 578586	—	—	—	—	MK177028
A. melissa	JHT3235	USNM 578687	MW177744	MW177727	MW177732	MW177723	MK177029
A. melissa	JHT3236	USNM 578688	—	—	—	—	MK177030
A. melissa	JHT3154	USNM 578682	—	—	—	—	MK177025
A. melissa	JHT3170	USNM 578683	—	—	—	—	MK177026
A. melissa	JHT2441	UF 166704	MK177062	MK177069	MW177733	MK176938	MK176947
A. panchoi	—	USAC 4608	MH004172	—	MH004197	MH004056	MH004056
A. spinipollex	CAC012	USNM 578664	MK177062	MK177070	MW177734	MK176939	MK176948
A. spinipollex	—	USNM 509525	AY819138	—	—	MH004057	MH004057
A. spinipollex	—	USNM 514381	—	AY844735	—	AY843748	AY843748
A. spinipollex	—	UTA A—50561	—	—	—	MH004058	MH004058
A. spinipollex	MMF192	CM 163344	—	—	—	—	MK177042
A. spinipollex	JHT3439	CM 170530	—	—	—	—	MK177031
A. spinipollex	JHT3440	CM 170529	—	—	—	—	MK177032

Appendix 1 continued.

Taxon	Field ID	Museum ID	POMC	RHO	RAG1	12S	16S
A. spinipollex	JHT3459	CM 170519	—	—	—	—	MK177033
A. spinipollex	JHT3460	CM 170520	MK177063	MK177071	MW177735	MK176940	MK176949
A. spinipollex	JHT3461	CM 170521	—	—	—	—	MK177034
A. spinipollex	JHT3462	CM 170522	—	—	—	—	MK177035
A. spinipollex	JHT3463	CM 170523	—	—	—	—	MK177036
A. spinipollex	JHT3464	CM 170524	—	—	—	—	MK177037
A. spinipollex	JHT3465	CM 170525	—	—	—	—	MK177038
A. spinipollex	JHT3472	CM 170526	—	—	—	—	MK177039
A. spinipollex	JHT3473	CM 170527	—	—	—	—	MK177040
A. spinipollex	JHT3474	CM 170528	—	—	—	—	MK177041
D. salvadorensis	JHT2262	UF 166696	MK177064	MK177072	MW177736	MK176941	MK176950
D. salvadorensis	JHT3704	CM 170641	MW177745	MK177076	MW177737	MK176945	MK176954
D. salvadorensis	—	USNM 563959	DQ055810	MH004221	MH004205	MH004067	MH004067
D. salvavida	—	USNM 559741	—	—	MH004202	MH004063	MH004064
D. salvavida	CAC009	USNM 578645	—	—	—	—	MK177043
D. salvavida	CAC010	USNM 578646	—	—	—	—	MK177044
D. salvavida	JHT3107	USNM 578647	MK177067	MK177075	MW177738	MK176944	MK176953
D. salvavida	JHT3108	USNM 578648	—	—	—	—	MK177045
D. salvavida	JHT3109	USNM 578649	—	—	—	—	MK177046
D. salvavida	JHT3110	USNM 578650	—	—	—	—	MK177047
D. salvavida	JHT3112	USNM 578652	—	—	—	—	MK177048
D. salvavida	JHT3141	USNM 578654	—	—	—	—	MK177049
D. salvavida	JHT3239	USNM 578655	—	—	—	—	MK177050
D. salvavida	JHT3327	USNM 578656	—	—	—	—	MK177051
D. salvavida	JHT3328	USNM 578657	MW177746	MW177728	MW177739	MW177724	MK177052
D. salvavida	JHT3329	USNM 578658	—	—	—	—	MK177053
D. salvavida	MMF193	CM 163345	—	—	—	—	MK177055
D. salvavida	MMF194	CM 163346	—	—	—	—	MK177056
D. salvavida	MMF195	CM 163347	—	—	—	—	MK177057
D. salvavida	MMF196	CM 163348	—	—	—	—	MK177058
D. salvavida	MMF197	CM 163349	—	—	—	—	MK177059
D. salvavida	JHT3468	CM 163201	—	—	—	—	MK177054
D. soralia	JHT1585	UF 147627	MW177747	MW177729	MW177740	MW177725	MK177060
D. soralia	—	USNM 570489	—	MH004222	—	MH004068	MH004068
D. soralia	—	UTA A-50812	AY819111	AY844557	AY844378	AY819362	AY819493
P. dendrophasma	—	UTA A-51838	DQ055790	AY844603	AY844414	AY843623	AY843623
P. euthysanota	JS1244	—	—	—	—	—	MK177008
P. euthysanota	—	USAC 3629	MH004188	—	MH004214	MH004096	MH004096
P. euthysanota	—	USAC 4613	MH004189	—	MH004215	MH004097	MH004097
P. euthysanota	—	UTA A-54786	—	AY844731	AY844509	AY843744	AY843744
P. hypomykter	IRL067	—	—	—	—	—	MK176955
P. hypomykter	IRL089	—	—	—	—	—	MK176956
P. hypomykter	IRL090	—	—	—	—	—	MK176957
P. hypomykter	IRL091	—	—	—	—	—	MK176958
P. hypomykter	IRL092	—	—	—	—	—	MK176959
P. hypomykter	IRL093	—	—	—	—	—	MK176960
P. hypomykter	IRL094	—	—	—	—	—	MK176961
P. hypomykter	IRL095	—	—	—	—	—	MK176962
P. hypomykter	JHT1622	UF 147625	—	—	—	—	MK176963
P. hypomykter	JHT2272	—	—	—	—	—	MK176964
P. hypomykter	JHT2273	—	—	—	—	—	MK176965
P. hypomykter	JHT2274	—	—	—	—	—	MK176966
P. hypomykter	JHT2275	—	—	—	—	—	MK176967
P. hypomykter	JHT2276	—	—	—	—	—	MK176968
P. hypomykter	JHT2299	UF 166698	—	—	—	—	MK176969
P. hypomykter	JHT2300	UF 166700	—	—	—	—	MK176970
P. hypomykter	JHT2494	UF 166699	—	—	—	—	MK176971
P. hypomykter	JHT2530	UF 166703	—	—	—	—	MK176972

Appendix 1 continued.

Taxon	Field ID	Museum ID	POMC	RHO	RAG1	12S	16S
P. hypomykter	JHT2540	UF 166701	—	—	—	—	MK176973
P. hypomykter	JHT2541	UF 166702	—	—	—	—	MK176974
P. hypomykter	JHT2548	—	—	—	—	—	MK176975
P. hypomykter	JHT2788	—	MK177065	MK177073	MW177741	MK176942	MK176951
P. hypomykter	JHT2855	—	MK177066	MK177074	MW177742	MK176943	MK176952
P. hypomykter	JHT2916	—	—	—	—	—	MK176976
P. hypomykter	JHT2930	—	—	—	—	—	MK176977
P. hypomykter	JHT2931	—	—	—	—	—	MK176978
P. hypomykter	JHT2932	—	—	—	—	—	MK176979
P. hypomykter	JHT2933	—	—	—	—	—	MK176980
P. hypomykter	JHT2934	—	—	—	—	—	MK176981
P. hypomykter	JHT2935	—	—	—	—	—	MK176982
P. hypomykter	JHT2936	—	—	—	—	—	MK176983
P. hypomykter	JHT2945	—	—	—	—	—	MK176984
P. hypomykter	JHT2946	—	—	—	—	—	MK176985
P. hypomykter	JHT2949	—	—	—	—	—	MK176986
P. hypomykter	JHT2950	—	—	—	—	—	MK176987
P. hypomykter	JHT2951	—	—	—	—	—	MK176988
P. hypomykter	JHT2952	—	—	—	—	—	MK176989
P. hypomykter	JHT2953	—	—	—	—	—	MK176990
P. hypomykter	JHT2954	—	—	—	—	—	MK176991
P. hypomykter	JHT2998	USNM 578662	—	—	—	—	MK176992
P. hypomykter	JHT2999	USNM 578663	—	—	—	—	MK176993
P. hypomykter	JHT3382	CM 163267	—	—	—	—	MK176994
P. hypomykter	JHT3383	CM 163268	—	—	—	—	MK176995
P. hypomykter	JHT3419	CM 163269	—	—	—	—	MK176996
P. hypomykter	MMF103	—	—	—	—	—	MK176997
P. hypomykter	N1000	UF 156120	—	—	—	—	MK176998
P. hypomykter	N1004	UF 156122	—	—	—	—	MK176999
P. hypomykter	N1028	UF 156125	—	—	—	—	MK177000
P. hypomykter	N242	UF 156406	—	—	—	—	MK177001
P. hypomykter	N293	—	—	—	—	—	MK177002
P. hypomykter	N528	UF 156413	—	—	—	—	MK177003
P. hypomykter	N547	UF 156115	—	—	—	—	MK177004
P. hypomykter	N606	UF 156389	—	—	—	—	MK177005
P. hypomykter	N626	UF 156116	—	—	—	—	MK177006
P. hypomykter	N993	UF 156119	—	—	—		MK177007
P. hypomykter	—	USNM 563952	—	MH004232	—	MH004099	MH004099
P. hypomykter	—	USNM 570496	—	MH004233	—	MH004100	MH004100
P. cf. hypomykter	—	UTA A-51040	DQ055809	—	—	AY819445	MH004098
P. cf. hypomykter	—	UTA A-51088	—	AY844732	—	AY843745	AY843745
P. leonhardschultzei	—	SMF 96519	—	—	—	MH004101	KX423519
P. leonhardschultzei	—	SMF 96522	—	—	—	MH004103	KX423521
P. leonhardschultzei	—	UTA A-54782	—	AY844733	—	AY843746	AY843746
P. macrotympanum	—	USAC 2475	MH004190	—	MH004216	MH004105	MH004105
P. macrotympanum	—	USAC 2479	MH004191	—	MH004217	MH004106	MH004106
P. sp.	—	JAC21606	—	AY844734	AY844511	AY843747	AY843747
P. zophodes	—	UTA A-54784	—	AY844736	AY844513	AY843749	AY843749

Appendix 2. Principal component scores for the first ten PCs from male and female morphological measurement analyses; acronyms used: snout-vent length (SVL), shank length (SHL; hind limb segment between the knee and the heel), foot length (FL; distance from posterior-most portion of inner metatarsal tubercle to tip of longest toe), head length (HL; tip of snout to posterior angle of jaw), head width (HW; greatest width), width of upper eyelid (EW; perpendicular to outer edge of eyelid), inter-orbital distance (IOD; measured at midlength of upper eyelids), tympanum length (TPL), eye length (EL; horizontal length of eye at widest point, measured inside margin of eyelid), and third finger disc width (DW; measured ventrally at widest point between outer edges of disc covers).

MALES	**PC1**	**PC2**	**PC3**	**PC4**	**PC5**	**PC6**	**PC7**	**PC8**	**PC9**	**P10**
St. Dev.	2.568	1.044	0.898	0.646	0.614	0.504	0.468	0.375	0.241	0.208
Prop. Var.	0.660	0.109	0.081	0.042	0.038	0.025	0.022	0.014	0.006	0.004
Cmlt. Prop.	0.660	0.769	0.849	0.891	0.929	0.954	0.976	0.990	0.996	1.000
SVL	– 0.344	0.056	– 0.099	0.435	– 0.118	0.476	– 0.445	0.295	0.386	– 0.071
SHL/SVL	0.362	– 0.014	0.034	– 0.210	– 0.101	– 0.275	– 0.020	0.783	0.205	– 0.285
FL/SVL	0.316	0.041	0.064	0.788	– 0.327	– 0.354	0.091	– 0.120	– 0.081	– 0.110
HL/SVL	0.370	0.034	0.064	– 0.036	0.166	0.245	0.289	– 0.358	0.681	– 0.305
HW/SVL	0.377	0.140	– 0.029	0.004	– 0.047	0.023	– 0.087	0.078	0.261	0.868
EW/SVL	0.140	– 0.571	– 0.793	0.088	0.125	– 0.001	0.046	0.008	– 0.006	0.017
TPL/SVL	0.338	0.156	0.074	0.257	0.529	0.479	0.163	0.255	– 0.434	– 0.031
IOD/SVL	0.330	– 0.015	– 0.072	– 0.243	– 0.694	0.496	– 0.051	– 0.100	– 0.273	– 0.107
EL/SVL	0.344	0.165	– 0.083	– 0.100	0.243	– 0.169	– 0.795	– 0.275	– 0.084	– 0.190
FDW/SVL	0.102	– 0.772	0.577	0.047	0.054	0.087	– 0.200	– 0.012	0.001	0.081
FEMALES	**PC1**	**PC2**	**PC3**	**PC4**	**PC5**	**PC6**	**PC7**	**PC8**	**PC9**	**P10**
St. Dev.	2.583	1.245	0.774	0.620	0.487	0.464	0.373	0.312	0.278	0.170
Prop. Var.	0.667	0.155	0.060	0.038	0.024	0.022	0.014	0.010	0.008	0.003
Cmlt. Prop.	0.667	0.822	0.882	0.920	0.944	0.966	0.980	0.989	0.997	1.000
SVL	0.326	– 0.364	0.072	– 0.136	0.033	– 0.123	0.389	0.710	– 0.201	– 0.160
SHL/SVL	– 0.360	– 0.082	– 0.362	– 0.048	– 0.163	0.012	– 0.122	– 0.071	– 0.615	– 0.553
FL/SVL	– 0.240	– 0.501	– 0.492	– 0.244	0.378	0.038	0.327	– 0.231	0.262	0.129
HL/SVL	– 0.370	– 0.061	– 0.065	0.107	– 0.030	0.001	– 0.369	0.459	0.606	– 0.359
HW/SVL	– 0.368	– 0.130	– 0.131	0.209	– 0.028	0.088	– 0.247	0.374	– 0.314	0.692
EW/SVL	– 0.313	0.007	0.570	– 0.412	0.471	0.385	– 0.078	0.035	– 0.155	– 0.080
TPL/SVL	– 0.342	0.027	0.266	0.044	0.200	– 0.868	0.086	– 0.067	– 0.060	0.019
IOD/SVL	– 0.335	0.120	0.094	– 0.514	– 0.671	0.007	0.327	0.033	0.138	0.151
EL/SVL	– 0.327	0.224	0.090	0.587	0.060	0.262	0.635	0.044	0.020	– 0.110
FDW/SVL	– 0.032	– 0.724	0.433	0.291	– 0.334	0.072	– 0.079	– 0.279	0.020	– 0.050